HBV/G has been detected in 25 of the 104 (24%) French patients coinfected with HIV-1 and HBV and was associated with a high risk of fibrosis at an odds ratio of 12.6.[22]

Mice with severe combined immunodeficiency disease (SCID) transgenic for the urokinase-type plasminogen activator gene under control of albumin promoter (uPA/SCID mice) have received human hepatocyte transplants.[23-25] These mice [hereafter referred to as chimeric (ChiM) mice] have been instrumental in experiments with hepatitis viruses *in vivo*[26,27] and offer a rare opportunity in portraying the early kinetics of HBV replication,[28] without having to resort to the ever-endangered species of chimpanzees. In this study, ChiM mice were monoinfected with HBV/G or coinfected with other genotypes, either simultaneously or in sequence, and followed for circulating HBV/G DNA. It is hoped that the emerging dynamics of HBV DNA will further characterize the dependence of HBV/G on other genotypes and unfold the pathogenicity intrinsic to this parasitic genotype.

Patients and Methods

Patients. Sera were obtained from 4 patients with chronic hepatitis B. One HBV DNA clone of subgenotype A2 and two of HBV/C2 were recovered from 3 Japanese patients in our recent study.[28] Because all HBV DNA clones of HBV/A were classified into subgenotype A2, they will be called HBV/A comprehensively in the present study. The other HBV/A and G clones were obtained from a coinfected Caucasian patient in San Francisco who represented patient 1 in our previous study.[17] All the HBV/A or C clones did not have precore or core promoter mutations affecting the expression of HBeAg. The study design conformed to the 1975 Declaration of Helsinki and was approved by the institutional ethics committees. Written informed consent was obtained from each patient.

Plasmid Constructs of HBV DNA and Sequencing. HBV DNA was extracted from 100 μL of serum using the QIAamp DNA blood kit (Qiagen, GmbH, Hilden, Germany). Four primer sets were designed for amplification of 2 fragments (A and B) covering the entire HBV/G genome. PCR with nested primers was performed with TaKaRa LA Taq polymerase (Takara Biochemicals, Kyoto, Japan) for 35 cycles (30 s at 95°C; 30 s at 60°C; 2 min at 72°C). Primer pairs and protocols for plasmid construction were described in supporting information. As reported previously,[28] these fragments were constructed into the pUC19 vector deprived of promoters (Invitrogen Corp., Carlsbad, CA) by digestion with *Hin*dIII and *Eco*RI, resulting in 1.24-fold the HBV genome—just enough to transcribe oversized pregenome and precore messenger RNA. Cloned HBV DNA sequences were confirmed with Prism BigDye (Applied Biosystems, Foster City, CA) using the ABI 3100 automated sequencer. Additionally, HBV DNA spanning the complete genome were amplified in mouse sera, cloned in the pGEM-T Easy Vector, and then sequenced.

Cell Culture and Transfection. Huh7 cells were transfected with plasmids equivalent to 5 μg of HBV DNA constructs with use of the Fugene 6 transfection reagent (Roche Diagnostics, Indianapolis, IN), and harvested after 3 days in culture. Transfection efficiency was monitored by 0.5 μg of coinfecting reporter plasmids expressing secreted alkaline phosphatase to estimate the latter's enzymatic activity in the culture supernatant.

Determination of HBV Markers. Hepatitis B surface antigen (HBsAg) and HBeAg were determined via chemiluminescent enzyme immunoassay using commercial assay kits (Fujirebio Inc., Tokyo, Japan). HBV core-related antigens (HBcrAg) were measured in serum using the chemiluminescent enzyme immunoassay described previously.[29,30]

Detection and Quantification of Serum HBV DNA. HBV DNA sequences spanning the S gene were determined via real-time detection PCR according to the method of Abe et al.[31] It had a sensitivity of 100 copies/ml (equivalent to 20 IU/ml) on the assay curve obtained with a calibrated World Health Organization standard serum containing HBV of genotype A (kindly provided by Dr. Hiroshi Yoshizawa of Hiroshima University) when 100 μl of the test sample was used. However, in assays for HBV DNA in mouse sera, in which only 10 μl of sample is used, the sensitivity decreased to 1,000 copies/ml (200 IU/ml). For real-time detection PCR specific for HBV/G, 10 μl of DNA sample was amplified in a 25-μl mixture containing 2 × SYBR Green PCR Master Mix (Applied Biosystems) and 2 primers specific for HBV/G: a forward primer (HBVG1620F: ACG TTA CAT GGA AAC CGC CA) and reverse primer (HBVHKR2: AGC CAA AAA GGC CAT ATG GCA) covering the 36–base pair insertion characteristic of this genotype.[5,16] Amplification and detection were performed in the ABI Prism 7700 Sequence Detection System (Applied Biosystems) with an initial activation of UNG at 50°C for 2 minutes, followed by incubation at 95°C for 10 minutes and subsequently, 40 three-step cycles (30 s at 95°C; 30 s at 60°C; 1 min at 72°C) were performed. The standard was prepared on serial dilutions of a known amount of the cloned HBV plasmid of HBV/G. The specificity of 2 primers (HBVG1620F and HBVHKR2) was confirmed in every PCR run via dissociation curve analysis (ABI Prism 7700 dissociation curve software; Applied Biosystems). The

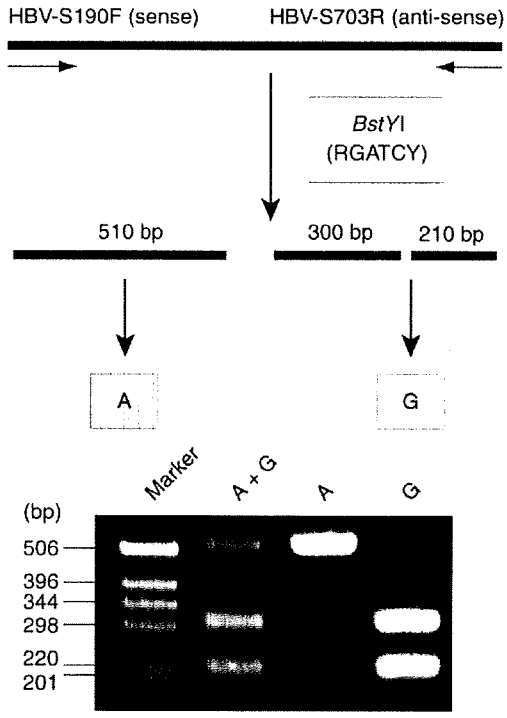

Fig. 1. PCR-RFLP for distinguishing between genotypes A and G. Products of PCR, when digested with *Bst*YI, split into 2 fragments for genotype G (upper panel). Infection with genotype A or G, or coinfection with these genotypes, can be determined by analyzing the patterns of electrophoresis of digests (lower panel).

sensitivity of detecting HBV/G via real-time detection PCR was 1000 copies/ml (200 IU/ml).

PCR Restriction Fragment Length Polymorphism for Distinguishing HBV DNA of Genotype G from Others. A novel method for specific determination of HBV/G DNA in the presence of other genotypes has been developed. It involved single-cycle PCR followed by restriction fragment length polymorphism (RFLP) with an endonuclease having the restriction site specific for HBV/G (Fig. 1). PCR was performed with a forward primer (HBV-S190F: GCT CGT GTT ACA GGC GGG) and reverse primer (HBV-S703R: GAA CCA CTG AAC AAA TGG CAC TAG TA) within the S region. To distinguish HBV/G from other genotypes such as HBV/A and C, a portion (5 μl) of amplification products of 510 base pairs was digested with 5 U *Bst*YI (restriction site: RGATCY) at 60°C for 2 hours. Digests were run on electrophoresis in 3.0% agarose gel, stained with ethidium bromide and examined for their sizes under the ultraviolet light. The results were supported by another method (Supplementary Fig. 1).

Inoculation of Chimeric Mice with the Liver Repopulated for Human Hepatocytes. SCID mice transgenic for the urokinase-type plasminogen activator gene with the liver repopulated for human hepatocytes (chimeric mice) were purchased from Phoenix Bio Co., Ltd. (Hiroshima, Japan). Human serum albumin was measured via ELISA using commercial assay kits (Eiken Chemical Co. Ltd, Tokyo, Japan). They were inoculated with HBV recovered from culture supernatants of Huh7 cells transfected with plasmids constructed with 1.24-fold the HBV genome of genotype HBV/A, C, or G after the method previously reported.[28]

Histopathological Examination. Liver tissues were fixed in buffered formalin, embedded in paraffin, and stained with hematoxylin-eosin or Masson's trichrome. The fibrosis stage was evaluated by an expert pathologist (S. T.) who was blinded to the nature of inocula.

Results

ChiM Mice Monoinfected with HBV/G. Two ChiM mice (ChiM92-3 and ChiM184-4) received an inoculum containing approximately 10^5 copies of HBV/G (G_US1646 strain) and were followed for 12 and 24 weeks, respectively (Fig. 2A,B). HBV DNA remained in undetectable levels ($<10^3$ copies/ml) in them both, but they developed low levels of HBcrAg (1 kU/ml) 4 and 8 weeks after inoculation, respectively. Despite absence of detectable HBV DNA in the circulation, therefore, these mice had contracted infection with HBV/G in very low levels. Intrahepatic cccDNA (covalently closed circular DNA) was detected via PCR specific for it,[32] and HBV/G DNA was detected in hepatocytes via PCR with type-specific primers[33]; they attested to infection with HBV/G in them (data not shown).

Superinfection With HBV/A on Mice Infected with HBV/G. Two chimeric mice with occult infection with HBV/G received 10^5 copies of HBV/A2 of different strains (A2_JPN to ChiM93-4 and A2_USA to ChiM172-3) 10 weeks after initial inoculation with HBV/G (Fig. 3A,B). They both developed HBV DNA in serum in titers $>10^6$ copies/ml at week 17, 7 weeks after superinfection with HBV/A, accompanied by HBcrAg and HBsAg; HBeAg appeared soon thereafter at week 22. HBV DNA and antigens increased, peaked at week 26, and then decreased in exactly the same patterns. HBV/G DNA, which was determined via PCR with type-specific primers, developed 12 weeks after the inoculation at week 22. It increased rapidly, and after the peak, took the same time course as total HBV DNA in serum—it had replaced HBV/A in the two chimeric mice.

Genotypes of HBV in ChiM93-4 were determined at the appearance of HBV DNA (week 17), at peak (week 26), and at the end of observation (week 38) via PCR-

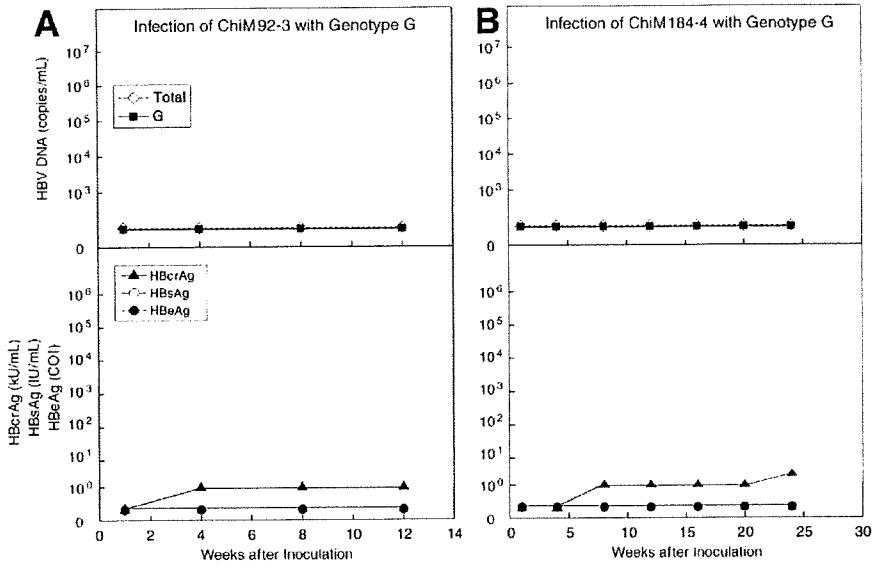

Fig. 2. (A) ChiM92-3 and (B) ChiM184-4 mice monoinfected with HBV/G. Profiles of total HBV DNA and HBV DNA of genotype G, determined via PCR with type-specific primers, are shown in the upper panels, and those of HBV antigens HBVcrAg, HBsAg, and HBeAg are shown in the lower panels. The shaded areas represent HBV DNA titers below the detection limit ($<10^3$ copies/ml).

RFLP (Fig. 3A). HBV/A accounted for all HBV DNA at week 17. At weeks 26 and 38, however, the vast majority of HBV DNA were of HBV/G with a trace of HBV/A. Thus, HBV/G needed coinfection with HBV/A for active replication, and took it over very swiftly.

Superinfection with HVB/G on Mice Infected with HBV/A. The chronological order of superinfection was reversed in ChiM92-9 and ChiM124-11 mice (Fig. 4A,B). The mice received 10^5 copies of HBV/A strains A2_JPN and A2_USA, respectively, and were superinfected with HBV/G (10^5 copies of G_US1646 strain) 10 weeks thereafter, when HBV/A DNA was elevated to $>5 \times 10^7$ copies/ml in both strains. Profiles of HBV DNA and antigens in these mice were quite similar but differed from those with A-on-G superinfection (Fig. 3A,B). HBV/A DNA was detected at week 1 in both groups and increased by approximately 2 logs within the next 3 weeks. HBV/G DNA developed within 3 weeks after superinfection with it, much sooner than the 12 weeks in ChiM mice superinfected with 2 genotypes in the reverse order. Three HBV antigens (HBcrAg, HBsAg, and HBeAg) waxed and waned in profiles similar to that of HBV DNA. HBV DNA levels decreased after they had peaked in ChiM92-9 as in A-on-G mice (Fig. 3A,B) by a margin close to log 2; the decrease was less prominent in ChiM124-11 by merely 1 log.

Composition of different genotypes in serum HBV DNA was followed in ChiM92-9 (Fig. 4A). Rapid replacement of HBV/A with HBV/G was obvious in G-on-A superinfection as in A-on-G superinfection (Fig. 3A). The takeover by HBV/G was not complete as in

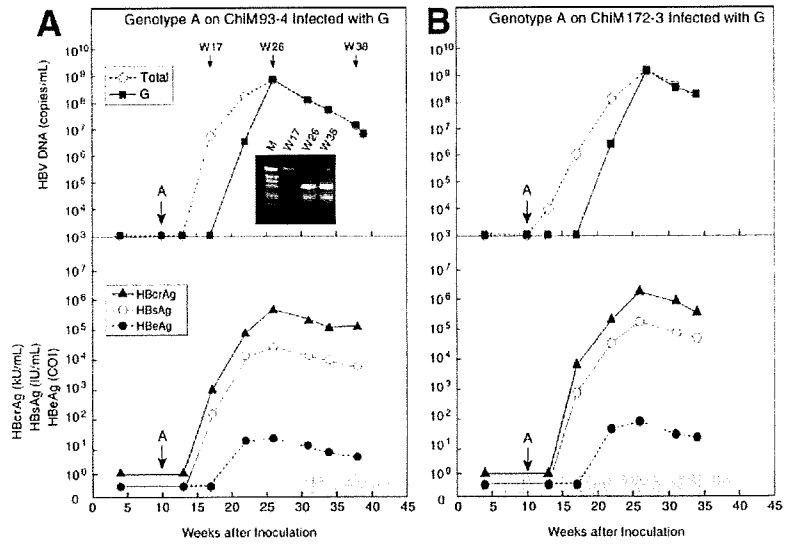

Fig. 3. Superinfection with HBV/A on (A) ChiM93-4 and (B) ChiM172-3 mice infected with HBV/G. Patterns of PCR-RFLP at different time points are shown in the insert in the upper panel of (A). Inoculation with genotype A is indicated by large arrows.

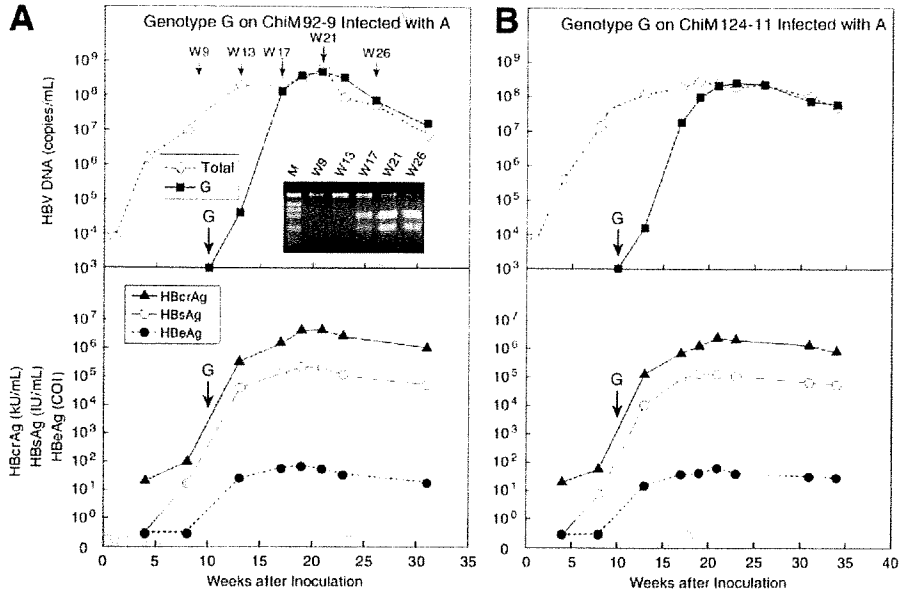

Fig. 4. Superinfection with HBV/G on (A) ChiM92-9 and (B) ChiM124-11 mice infected with HBV/A. Patterns of PCR-RFLP at different time points are shown in the insert in the upper panel of (A). Inoculation with genotype G is indicated by large arrows.

A-on-G superinfection, and HBV/A remained at very low levels throughout the weeks of observation.

Superinfection with HBV/G on Mice Infected with HBV/C. Similar superinfection with HBV/G was performed on ChiM mice that had been infected with HBV/C2 (Fig. 5A,B). Thus, C_22 and C_AT strains (10^5 copies) of HBV/C were injected intravenously into ChiM91-21 and ChiM95-11, respectively. They were superinfected with HBV/G (10^5 copies of G_US1646 strain) at week 10, when HBV DNA stabilized at approximately 10^9 copies/ml. HBV/G appeared in serum 3 weeks thereafter, at week 13 in both groups, and increased exponentially until weeks 21-23. The time required for an increase in HBV DNA level by 10-fold (log time) was 3.3 weeks in both groups, which was twice as long as the 1.6 weeks in mice with A-on-G and G-on-A superinfections (Figs. 3, 4). Likewise, the takeover of HBV/C by HBV/G in these mice was not as rapid or extensive as in superinfection with HBV/G on HBV/A (Figs. 3A, 4A, 5A). HBV antigens took time courses similar to that of HBV DNA, and they never waned after they had stabilized; however, mice were followed until 26 and 34 weeks.

Simultaneous Coinfection of Mice with HBV/A and HBV/G. Two ChiM mice (ChiM93-10 and ChiM93-

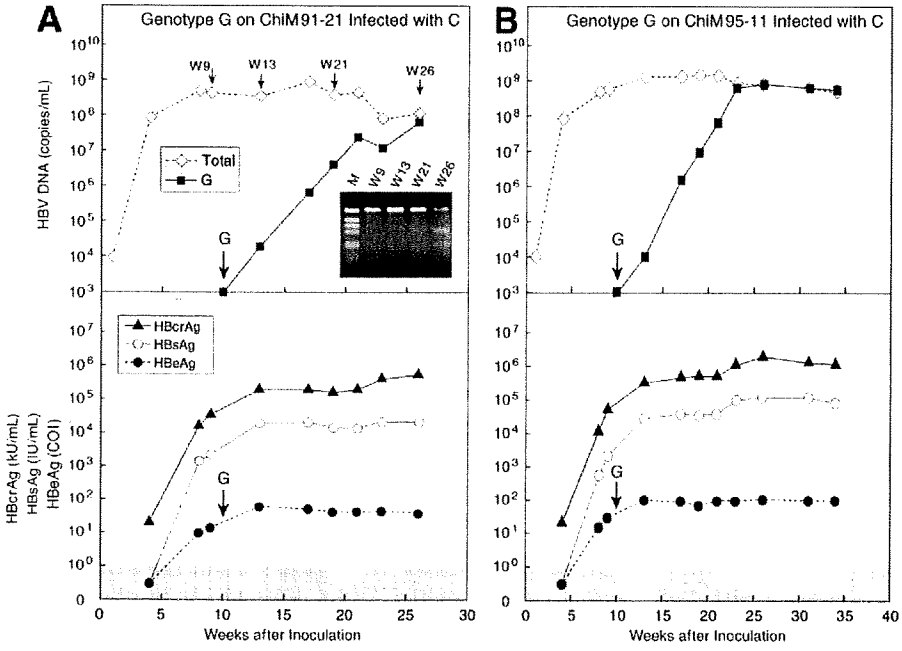

Fig. 5. Superinfection with HBV/G on (A) ChiM91-21 and (B) ChiM95-11 mice infected with HBV/C. Patterns of PCR-RFLP at different time points are shown in the insert the in upper panel of (A). Inoculation with genotype G is indicated by large arrows.

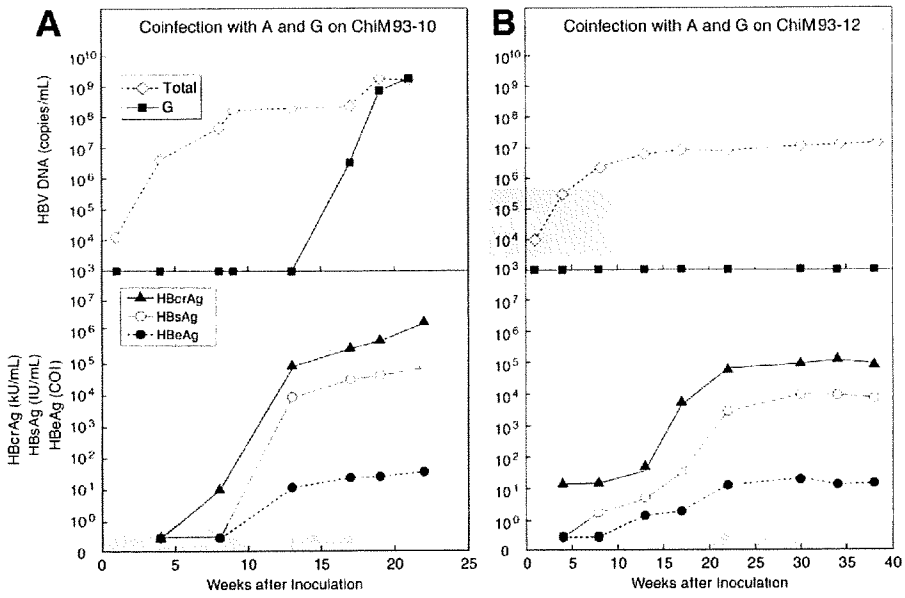

Fig. 6. (A) ChiM93-10 and (B) ChiM93-12 mice simultaneously infected with genotypes A and G.

12) received simultaneous inoculation with 10^5 copies each of HBV/A (A2_JPN strain) and HBV/G (G_US1646 strain). The ChiM93-10 mouse developed HBV/G DNA 17 weeks after inoculation, 9 weeks since HBV/A DNA had increased to $>10^7$ copies/ml (Fig. 6A). HBV/G DNA increased to the level of total HBV DNA at week 21, thereby indicating that by then, HBV/G had taken over HBV/A almost completely.

For the reasons unknown, infection with HBV/G was not established in the ChiM93-12 mouse simultaneously coinfected with HBV/A (Fig. 6B), although it was infected with HBV/A in levels by some 2 logs lower (10^7 copies/ml) than the ChiM93-10 mouse. Serum levels of human albumin in the ChiM93-12 mouse (mean, 2.1×10^6 ng/ml) were much lower than the other chimeric mice used in this study (mean, 4.7×10^6 ng/ml). Thus, a lower extent of repopulation with human hepatocytes may have prohibited active replication of HBV/A. This would be a prerequisite to infection with HBV/G at high levels.

Coinfection of Mice with HBV/A and HBV/G by Inoculation with a Mouse Passage of G-on-A Superinfection. Three ChiM mice (ChiM169-8, ChiM133-3, and ChiM133-6) received serum from a ChiM92-9 mouse with G-on-A superinfection taken at week 26, when HBV/G had almost replaced HBV/A (Fig. 3A). Profiles of HBV/A and HBV/G, after inoculation with 10^5 copies of HBV DNA, were similar among the mice (Fig. 7A-C). HBV/G DNA was detected at week 1 in levels comparable to those of total HBV DNA. Despite receiving the inoculation with a mouse passage containing HBV/G, in copies by 5 logs greater than those of HBV/A, HBV/G DNA decreased thereafter and stayed >1 log lower than total HBV DNA until week 7. Since week 4, HBV/G started to increase and replaced HBV/A almost completely until weeks 10-12, and continued to do so through weeks 19-22 of the observation (Fig. 7A).

Cloning and Sequencing HBV DNA in Chimeric Mice Coinfected with HBV/A and HBV/G. HBV DNA clones from sera of ChiM92-9 sampled at 26 weeks (Fig. 4A) and ChiM169-8 inoculated with serum passage in it (Fig. 7A) included those of HBV/A and G invariably. They confirmed the results of real-time detection PCR and PCR-RFLP and did not possess any mutations in comparison with the original inoculum of either genotype. No recombinations between HBV/A and G were detected, either. At least 5 clones of each genotype were propagated and sequenced in both sera.

Cotransfection of Huh7 Cells with Plasmids Carrying the Core Gene of Genotype A and the Entire Genome of Genotype G. Huh7 cells were transfected with 2 plasmids that were pcDNA_core clones that expressed the core protein of genotype A2, under the control of cytomegalovirus promoter, and the pUC19/G clone incorporated with 1.24-fold the genome of genotype G. Transfection only with genotype G induced its replication in a weak level (Fig. 8). When Huh7 cells were cotransfected with the genotype G clone and the genotype A core clone, however, the replication was enhanced in a dose-dependent manner.

Liver Pathology of ChiM Mice Infected with HBV/A and/or HBV/G. Figure 9 shows the histology of liver in representative ChiM mice either simultaneously coinfected with genotypes A and G (viremia of only ge-

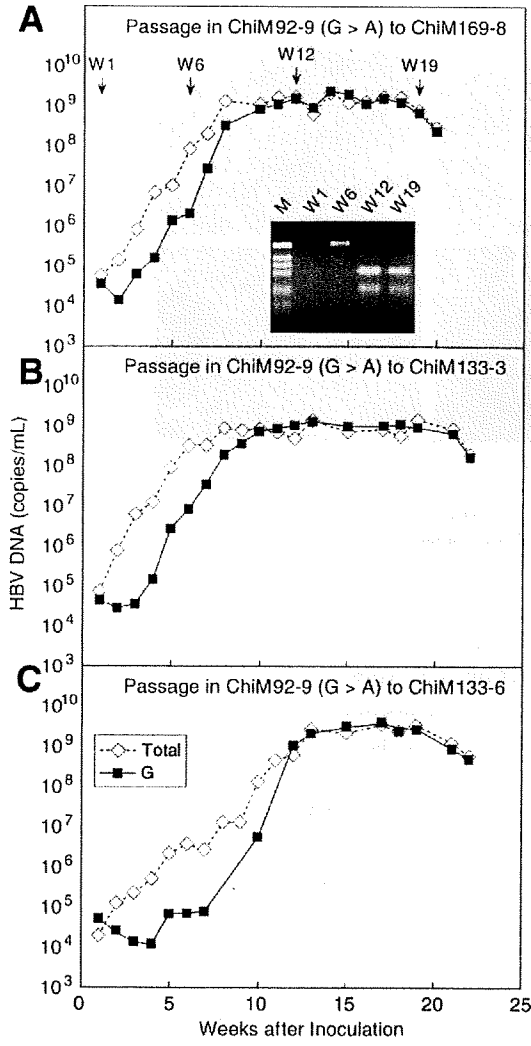

Fig. 7. (A) ChiM169-8, (B) ChiM133-3, and (C) ChiM133-6 mice inoculated with a serum passage from a mouse coinfected with genotypes A and G (ChiM92-9 in Fig. 4A).

notype A in ChiM93-12) or superinfected with genotypes G-on-A (ChiM92-9) and monoinfected with genotype G (ChiM92-3) during 32-39 weeks. HBV infection was demonstrated by double staining for HBcAg and human albumin (Supplementary Fig. 2). The mouse coinfected with genotypes A and G revealed steatosis of hepatocytes with hematoxylin-eosin stain and fibrosis of stage 2 (F2) with Masson's trichrome stain. In contrast, the mice monoinfected with genotype A (ChiM93-12) or G (ChiM92-3) had neither steatosis nor fibrosis. Table 1 summarizes the liver pathology of all autopsied mice. Steatosis in 30%-80% of repopulated human hepatocytes and stage F1-F2 fibrosis were observed in the majority of mice superinfected or coinfected with genotypes G and A or C.

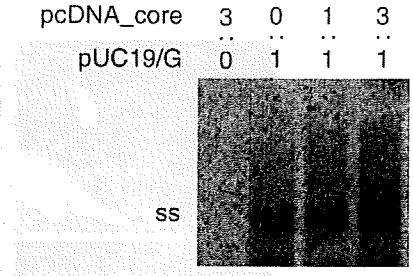

Fig. 8. *Trans*-complementation of the core gene of genotype A for enhanced replication of genotype G. Huh7 cells were cotransfected with plasmids constructed with 1.24-fold the genome of genotype G (pUC19/G) and plasmids expressing the core gene of genotype A (pcDNA_core) in an increasing ratio. Gel strips were Southern-blotted by the complete HBV probe of genotype G. The far left lane represents negative control with pcDNA_core alone. The migration position of single-stranded (ss) HBV DNA is indicated on the left.

Discussion

Using ChiM mice infected with pedigreed HBV DNA in the standardized copy number, we have determined early viral dynamics of HBV/G in detail. Due to constraints on securing ChiM mice with a satisfactory rate of replacement for human hepatocytes (>60%), only 2 or 3 of them were used for each experiment. Concordance of viral dynamics among them, however, would give credence to the reproducibility of obtained results.

HBV/G infected ChiM mice by itself in corroboration with its monoinfection in human beings.[21] The replication was very slow, however, and did not elevate serum HBV DNA to levels detectable by the method used (>10^3 copies/ml). Coinfection with HBV/A enhanced the replication of HBV/G remarkably. HBV/G replicated vividly when coinfected with HBV/C, as well. However, the time required for a 10-fold increase (log time) is 2-fold longer in mice initially infected with HBV/C versus HBV/A (3.3 versus 1.6 weeks). Combined, these results would indicate that HBV/G can thrive at the expense of other genotypes, and coinfection with HBV/A is much more advantageous for its enhanced replication than the other genotypes, including HBV/C. In support of this view, coinfection with HBV/A is frequent in individuals infected with HBV/G.[16,34] Such a heavy dependence of HBV/G on HBV/A does not require recombination between them, because no recombination events occurred in ChiM mice coinfected with them.

The initial replication of HBV/G was much slower than that of HBV/A, even in simultaneous coinfection. This was typically observed in three ChiM mice inoculated with a mouse passage of G-on-A superinfection containing HBV/G in the concentration a few logs higher than that of HBV/A. Despite such an enormous difference in introduced virions, the replication of HBV/A far

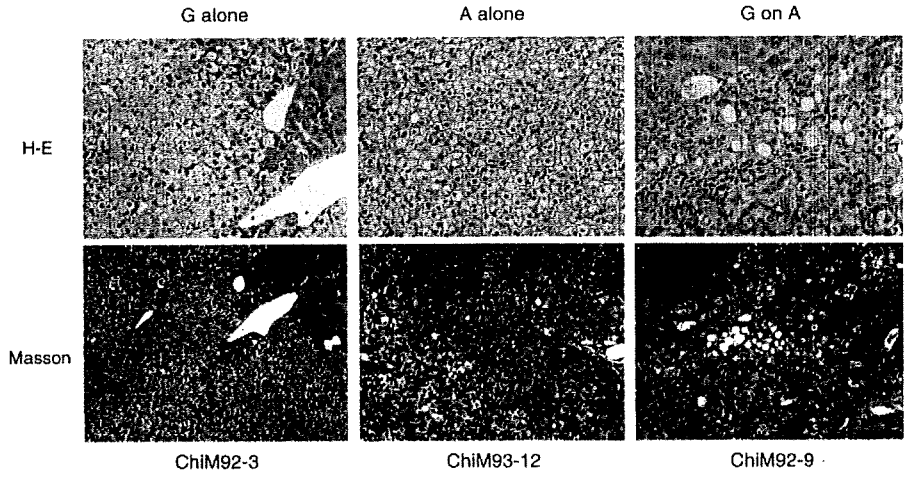

Fig. 9. Liver histology in a ChiM92-3 mouse monoinfected with genotype G, a ChiM93-12 mouse coinfected with genotypes A and G (but persistently infected with genotype A alone), and a ChiM92-9 mouse superinfected with genotype G-on-A. Liver sections stained with hematoxylin-eosin or Masson's trichrome stain are shown.

exceeded that of HBV/G in the initial several weeks. Thereafter, HBV/G caught up with HBV/A, then took it over almost completely. Such a replacement was observed when HBV/G was superinfected on HBV/A, or vice versa.

The mechanism by which genotype G depends on genotype A for replication was pursued in cotransfection experiments in Huh7 cells. Cotransfection with the pcDNA_core clone carrying the core gene of genotype A2 increased the replication of the pUC19/G clone constructed with 1.24-fold the genome of genotype G in a dose-dependent manner (Fig. 8). Hence, *trans*-complementation with the core protein of genotype A would be required for genotype G to replicate actively. The possibility remains, however, for other viral elements from coinfecting genotypes to enhance the replication of genotype G. Cotransfection of cultured cells with genotype G and others would help clarify how it depends on coinfecting the other genotypes.[35]

Table 1. Steatosis and Fibrosis in Human Hepatocytes in the Liver of Chimeric Mice Monoinfected or Coinfected with HBV/G

		Features	
Inoculation	Mouse No.	Steatosis (%)*	Fibrosis Stage
G alone	ChiM92-3	<5	F0
	ChiM 184-4	<5	F0
A alone	ChiM 93-12†	<5	F0
A-on-G	ChiM 93-4	50	F1
	ChiM 172-3	40	F1
G-on-A	ChiM 92-9	40	F2
	ChiM 124-11	50	F1
G-on-C	ChiM 91-21	80	F2
	ChiM 95-11	NA	NA
A plus G	ChiM 93-10	30	F0
Passage	ChiM 169-8	50	F1
A plus G	ChiM 133-3	<5	F2
	ChiM 133-6	30	F2

Abbreviation: NA, not available.

*Percentage of human hepatocytes with steatosis. †Simultaneously inoculated with A plus G but became infected with genotype A only (Fig. 6B).

Coinfection with HBV/G may be associated with pathological manifestations. ChiM mice coinfected with HBV/A and HBV/G developed steatosis and fibrosis in the liver not observed in mice monoinfected with either of these genotypes. Very recently, Lacombe et al.[22] reported more severe fibrosis in HIV-positive French patients who were infected with HBV/G than the others; they would most likely have been coinfected with other genotypes in undetectable levels. On the basis of clinical and experimental pieces of evidence, it does seem that HBV/G has a strong disease-inducing capacity, which would be operable only when it is coinfected with other genotypes. High levels of HBcrAg in mice with HBV/G (Figs. 3-6) under immunocompromised states would implicate accumulation of the product of the core gene in the fibrosis of patients coinfected with it and HIV. Patients with HIV are infected with HBV at a frequency of 6%-9%, and liver-related deaths happen more often in coinfected patients.[36,37] Fibrosis proceeds faster in patients coinfected with HIV and HBV, as in those with HCV.[38,39] Therapeutic intervention to prevent fibrosis would be required in patients coinfected with HIV and HBV, particularly in HBV/G patients.

In conclusion, the early viral dynamics of HBV/G have been characterized in ChiM mice monoinfected with HBV/G or coinfected with other genotypes. The replication of HBV/G is very slow and depends heavily on coinfection with other genotypes. HBV/G rapidly takes over

the other genotypes, though they are indispensable. Infection with HBV/G may induce steatosis and fibrosis in the liver—but again, only in the case of coinfection with other genotypes. However, it is still unclear whether or not such an increased pathogenicity of HBV/G is expressed exclusively in animals and patients with genetic or acquired immune deficiency.

References

1. Lee WM. Hepatitis B virus infection. N Engl J Med 1997;337:1733-1745.
2. Arauz-Ruiz P, Norder H, Robertson BH, Magnius LO. Genotype H: a new Amerindian genotype of hepatitis B virus revealed in Central America. J Gen Virol 2002;83:2059-2073.
3. Norder H, Hammas B, Lofdahl S, Courouce AM, Magnius LO. Comparison of the amino acid sequences of nine different serotypes of hepatitis B surface antigen and genomic classification of the corresponding hepatitis B virus strains. J Gen Virol 1992;73:1201-1208.
4. Okamoto H, Tsuda F, Sakugawa H, Sastrosoewignjo RI, Imai M, Miyakawa Y, et al. Typing hepatitis B virus by homology in nucleotide sequence: comparison of surface antigen subtypes. J Gen Virol 1988;69: 2575-2583.
5. Stuyver L, De Gendt S, Van Geyt C, Zoulim F, Fried M, Schinazi RF, et al. A new genotype of hepatitis B virus: complete genome and phylogenetic relatedness. J Gen Virol 2000;81:67-74.
6. Naumann H, Schaefer S, Yoshida CF, Gaspar AM, Repp R, Gerlich WH. Identification of a new hepatitis B virus (HBV) genotype from Brazil that expresses HBV surface antigen subtype adw4. J Gen Virol 1993;74:1627-1632.
7. Miyakawa Y, Mizokami M. Classifying hepatitis B virus genotypes. Intervirology 2003;46:329-338.
8. Schaefer S. Hepatitis B virus: significance of genotypes. J Viral Hepat 2005;12:111-124.
9. Chu CJ, Lok AS. Clinical significance of hepatitis B virus genotypes. HEPATOLOGY 2002;35:1274-1276.
10. Liu CJ, Kao JH, Chen DS. Therapeutic implications of hepatitis B virus genotypes. Liver Int 2005;25:1097-1107.
11. Sugauchi F, Kumada H, Sakugawa H, Komatsu M, Niitsuma H, Watanabe H, et al. Two subtypes of genotype B (Ba and Bj) of hepatitis B virus in Japan. Clin Infect Dis 2004;38:1222-1228.
12. Tanaka Y, Orito E, Yuen MF, Mukaide M, Sugauchi F, Ito K, et al. Two subtypes (subgenotypes) of hepatitis B virus genotype C: A novel subtyping assay based on restriction fragment length polymorphism. Hepatol Res 2005;33:216-224.
13. Sugauchi F, Kumada H, Acharya SA, Shrestha SM, Gamutan MT, Khan M, et al. Epidemiological and sequence differences between two subtypes (Ae and Aa) of hepatitis B virus genotype A. J Gen Virol 2004;85:811-820.
14. Akuta N, Suzuki F, Kobayashi M, Tsubota A, Suzuki Y, Hosaka T, et al. The influence of hepatitis B virus genotype on the development of lamivudine resistance during long-term treatment. J Hepatol 2003;38:315-321.
15. Tanaka Y, Hasegawa I, Kato T, Orito E, Hirashima N, Acharya SK, et al. A case-control study for differences among hepatitis B virus infections of genotypes A (subtypes Aa and Ae) and D. HEPATOLOGY 2004;40:747-755.
16. Kato H, Orito E, Gish RG, Sugauchi F, Suzuki S, Ueda R, et al. Characteristics of hepatitis B virus isolates of genotype G and their phylogenetic differences from the other six genotypes (A through F). J Virol 2002;76:6131-6137.
17. Kato H, Orito E, Gish RG, Bzowej N, Newsom M, Sugauchi F, et al. Hepatitis B e antigen in sera from individuals infected with hepatitis B virus of genotype G. HEPATOLOGY 2002;35:922-929.
18. Perez-Olmeda M, Nunez M, Garcia-Samaniego J, Rios P, Gonzalez-Lahoz J, Soriano V. Distribution of hepatitis B virus genotypes in HIV-infected patients with chronic hepatitis B: therapeutic implications. AIDS Res Hum Retroviruses 2003;19:657-659.
19. Suwannakarn K, Tangkijvanich P, Theamboonlers A, Abe K, Poovorawan Y. A novel recombinant of hepatitis B virus genotypes G and C isolated from a Thai patient with hepatocellular carcinoma. J Gen Virol 2005;86:3027-3030.
20. Sanchez LV, Tanaka Y, Maldonado M, Mizokami M, Panduro A. Difference of hepatitis B virus genotype distribution in two groups of Mexican patients with different risk factors. High prevalence of genotype H and G. Intervirology 2007;50:9-15.
21. Chudy M, Schmidt M, Czudai V, Scheiblauer H, Nick S, Mosebach M, et al. Hepatitis B virus genotype G monoinfection and its transmission by blood components. HEPATOLOGY 2006;44:99-107.
22. Lacombe K, Massari V, Girard PM, Serfaty L, Gozlan J, Pialoux G, et al. Major role of hepatitis B genotypes in liver fibrosis during coinfection with HIV. AIDS 2006;20:419-427.
23. Heckel JL, Sandgren EP, Degen JL, Palmiter RD, Brinster RL. Neonatal bleeding in transgenic mice expressing urokinase-type plasminogen activator. Cell 1990;62:447-456.
24. Rhim JA, Sandgren EP, Degen JL, Palmiter RD, Brinster RL. Replacement of diseased mouse liver by hepatic cell transplantation. Science 1994; 263:1149-1152.
25. Tateno C, Yoshizane Y, Saito N, Kataoka M, Utoh R, Yamasaki C, et al. Near completely humanized liver in mice shows human-type metabolic responses to drugs. Am J Pathol 2004;165:901-912.
26. Mercer DF, Schiller DE, Elliott JF, Douglas DN, Hao C, Rinfret A, et al. Hepatitis C virus replication in mice with chimeric human livers. Nat Med 2001;7:927-933.
27. Tsuge M, Hiraga N, Takaishi H, Noguchi C, Oga H, Imamura M, et al. Infection of human hepatocyte chimeric mouse with genetically engineered hepatitis B virus. HEPATOLOGY 2005;42:1046-1054.
28. Sugiyama M, Tanaka Y, Kato T, Orito E, Ito K, Acharya SK, et al. Influence of hepatitis B virus genotypes on the intra- and extracellular expression of viral DNA and antigens. HEPATOLOGY 2006;44:915-924.
29. Kimura T, Ohno N, Terada N, Rokuhara A, Matsumoto A, Yagi S, et al. Hepatitis B virus DNA-negative dane particles lack core protein but contain a 22-kDa precore protein without C-terminal arginine-rich domain. J Biol Chem 2005;280:21713-21719.
30. Shinkai N, Tanaka Y, Orito E, Ito K, Ohno T, Hirashima N, et al. Measurement of hepatitis B virus core-related antigen as predicting factor for relapse after cessation of lamivudine therapy for chronic hepatitis B virus infection. Hepatol Res 2006;36:272-276.
31. Abe A, Inoue K, Tanaka T, Kato J, Kajiyama N, Kawaguchi R, et al. Quantitation of hepatitis B virus genomic DNA by real-time detection PCR. J Clin Microbiol 1999;37:2899-2903.
32. Mason AL, Xu L, Guo L, Kuhns M, Perrillo RP. Molecular basis for persistent hepatitis B virus infection in the liver after clearance of serum hepatitis B surface antigen. HEPATOLOGY 1998;27:1736-1742.
33. Kato H, Orito E, Sugauchi F, Ueda R, Gish RG, Usuda S, et al. Determination of hepatitis B virus genotype G by polymerase chain reaction with hemi-nested primers. J Virol Methods 2001;98:153-159.
34. Osiowy C, Giles E. Evaluation of the INNO-LiPA HBV genotyping assay for determination of hepatitis B virus genotype. J Clin Microbiol 2003;41: 5473-5477.
35. Kremsdorf D, Garreau F, Capel F, Petit MA, Brechot C. In vivo selection of a hepatitis B virus mutant with abnormal viral protein expression. J Gen Virol 1996;77:929-939.
36. Konopnicki D, Mocroft A, de Wit S, Antunes F, Ledergerber B, Katlama C, et al. Hepatitis B and HIV: prevalence, AIDS progression, response to highly active antiretroviral therapy and increased mortality in the EuroSIDA cohort. AIDS 2005;19:593-601.
37. Thio CL, Seaberg EC, Skolasky R Jr, Phair J, Visscher B, Munoz A, et al. HIV-1, hepatitis B virus, and risk of liver-related mortality in the Multicenter Cohort Study (MACS). Lancet 2002;360:1921-1926.
38. Benhamou Y, Bochet M, Di Martino V, Charlotte F, Azria F, Coutellier A, et al. Liver fibrosis progression in human immunodeficiency virus and hepatitis C virus coinfected patients. The Multivirc Group. HEPATOLOGY 1999;30:1054-1058.
39. Colin JF, Cazals-Hatem D, Loriot MA, Martinot-Peignoux M, Pham BN, Auperin A, et al. Influence of human immunodeficiency virus infection on chronic hepatitis B in homosexual men. HEPATOLOGY 1999;29:1306-1310.

[Autophagy 5:7, 937-945; 1 October 2009]; ©2009 Landes Bioscience

Clinical Brief Report

Knockdown of autophagy-related gene decreases the production of infectious hepatitis C virus particles

Isei Tanida,[1,2,*] Masayoshi Fukasawa,[1] Takashi Ueno,[2] Eiki Kominami,[2] Takaji Wakita[3] and Kentaro Hanada[1]

[1]Department of Biochemistry and Cell Biology; National Institute of Infectious Diseases; Toyama; Shinjyuku, Tokyo Japan; [2]Department of Biochemistry; Juntendo University School of Medicine; Tokyo, Japan; [3]Department of Virology II; National Institute of Infectious Diseases; Tokyo, Japan

Abbreviations: Atg, autophagy related genes and their products; Beclin 1, autophagy-related bcl2-interacting Atg6 homologue; BECN1, *beclin 1* gene and mRNA; HCV, hepatitis C virus; IFNA1, interferon alpha1 gene; IFNA2, interferon alpha2 gene; IFNB1, interferon beta1 gene; NS, nonstructural protein; LC3, wild-type human microtubule-associated protein 1 light chain 3; LC3-I, soluble unlipidated form of LC3; LC3-II, LC3-phospholipid conjugate

Key words: autophagy, Atg7, LC3, Beclin 1, Hepatitis C virus, infectious HCV particles

Hepatitis C virus (HCV) is a positive-strand RNA virus, and classified within the Flaviridae family. Atg7-knockdown decreases the amount of HCV replicon RNA, when HCV JFH1 RNA and HCV subgenomic replicon are transfected into Huh7.5 cells. However, when infectious naive HCV particles are directly infected into Huh7.5.1 cells, it is still unclear whether Atg7-knockdown decreases the production of intracellular HCV-related proteins, HCV mRNA and infectious HCV particles. When Atg7 protein in HCV-infected Huh7.5.1 cells was knocked down by RNA-interference, the levels of intracellular HCV core, NS3, NS5A proteins, HCV mRNA and secreted albumin remained unchanged compared with those in the control HCV-infected cells. However, the level of infectious HCV particles released in the medium was decreased by the Atg7-knockdown. Similar results were obtained when Beclin 1 was knocked down by RNA-interference. The colocalization of endogenous LC3-puncta with HCV core, HS5A proteins and lipid droplets was also investigated. However, little endogenous LC3-puncta colocalized with HCV core, NS5A proteins or lipid droplets. These results suggested that autophagy contributed to the effective production of HCV particles, but little to the intracellular production of HCV-related proteins, HCV mRNA and the secretory pathway, in a naive HCV particles-infection system.

*Correspondence to: Isei Tanida; Department of Biochemistry and Cell Biology; National Institute of Infectious Diseases; 1-23-1, Toyama, Shinjyuku, Tokyo 162-8640 Japan; Tel.: +81.3.5285.1111x2126; Fax: +81.3.5285.1157; Email: tanida@nih.go.jp

Submitted: 11/24/08; Revised: 06/10/09; Accepted: 06/10/09

Previously published online as an *Autophagy* E-publication: http://www.landesbioscience.com/journals/autophagy/article/9243

Introduction

Hepatitis C virus (HCV) is a positive-strand RNA virus with a genome size of 9.6 kb, and is classified within the Flaviridae family.[1] HCV is spread by blood-to-blood contact, and infection can lead to liver cirrhosis and heaptocellular carcinoma. More than 150 million people in the world are infected with HCV. The HCV genome encodes polyproteins that are processed into structural proteins (core protein and envelope glycoproteins) and nonstructural (NS) proteins (NS1-NS5A including a protease and RNA helicase).[2] HCV replicates in association with intracellular membrane structures called "the membranous web."[3] HCV-infected cells accumulate lipid droplets, and the lipid droplets play an important role in the assembly of HCV particles.[4] HCV core protein recruits NS proteins and replication complexes to lipid droplets-associated membranes. This recruitment is critical for producing infectious viruses.

Recently, when HCV JFH1 RNA and HCV subgenomic replicon were transfected into Huh7.5 cells, HCV infection leads to incomplete autophagic flux, and Atg7-knockdown decreases the amount of HCV replicon RNA.[5-7] Interestingly, endogenous LC3 can associate with cytoplasmic lipid droplets in uninfected Huh7.5.1 cells.[8] Considering that HCV core and NS5A proteins associate with lipid droplets for the assembly of HCV particles, it is possible that Atg7-knockdown will result in a decreased production of these particles. Therefore, the contribution of Atg7 to the production of intracellular HCV-related proteins and the release of infectious HCV particles was investigated. In addition, the authors investigated whether endogenous LC3 colocalizes to HCV lipid droplets, HCV core and NS5A proteins.

Results

Human *ATG7* and *BECN1* RNAi resulted in decreased release of HCV particles in the medium without a decrease of the intracellular production of HCV-related proteins and HCV

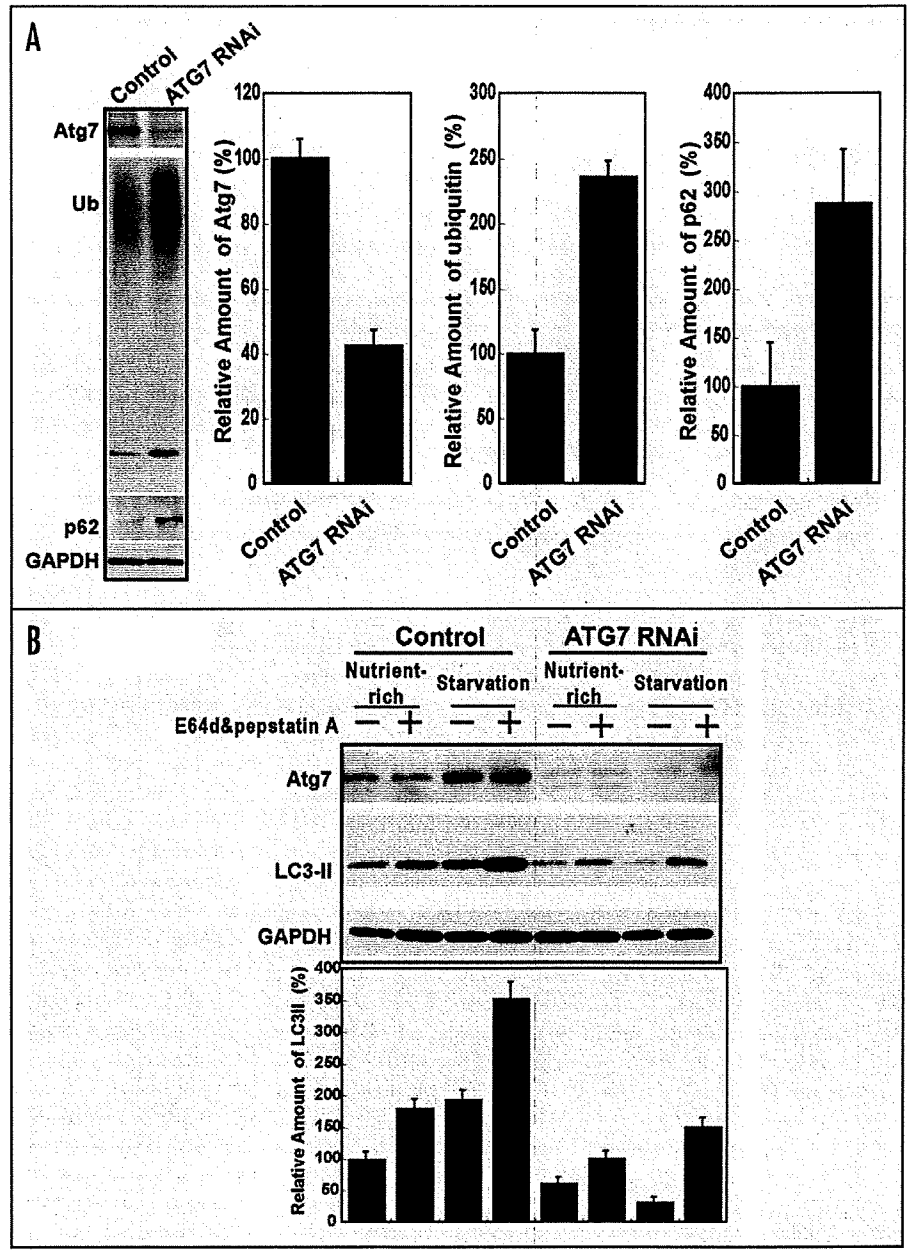

Figure 1. Effect of *ATG7*-RNAi on p62, ubiquitinated proteins and lysosomal turnover of LC3-II. (A) Increase of p62 and ubiquitinated proteins in Huh7 cells by *ATG7*-RNAi. dsRNA for *ATG7*-RNAi was transfected into Huh7.5.1 cells (ATG7 RNAi). As a negative control, scrambled dsRNA was employed (Control). Cells were harvested after incubation at 37°C for 48 h, and total proteins (20 μg) were separated on SDS-PAGE. Atg7, p62 and ubiquitinated proteins (ubiquitin) in the lysate were recognized by immunoblotting. GAPDH was employed as a loading control. Right: indicated the relative levels of intensity of each band of three independent experiments estimated by densitometry. Error bars indicate standard errors. (B) Effect of *ATG7*-RNAi on lysosomal turnover of LC3-II. Atg7-knockdown was performed as described in (A), and cells were cultured for 48 h. For Nutrient-rich conditions, cells were cultured in DMEM medium containing 10% FCS. Where indicated, cells were treated with the protease inhibitors, E64d (10 μg/ml) and pepstatin A (10 μg/ml) (E64d & pepstatin A +) for 4 h, or, as a negative control (Inhibitors -), with the solvent, dimethylsulfoxide. For Starvation conditions, cells were incubated for 4 hrs in Krebs-Ringer medium (KRB) in the presence (+) or absence (-) of the protease inhibitors. The cells were lysed, total proteins (10 μg per lane) were separated by SDS-PAGE, and endogenous LC3 and Atg7 in the lysates was recognized by immunoblotting. LC3-II, membrane-bound form of LC3. Lower: indicated the relative levels of intensity of each band estimated by densitometry. Error bars indicate standard errors.

mRNA. The initial investigation was on whether Atg7-knockdown leads to a decreased HCV core, NS3 and NS5A proteins in an in vitro naive HCV particle-infection system. Atg7 in Huh7.5.1 cells was knocked down by double-stranded RNAs for *ATG7* RNAi compared with scrambled double-stranded RNAs (Fig. 1A). The Atg7-knockdown in Huh7.5.1 cells resulted in an increase of p62 and ubiquitinated proteins (Fig. 1A), and led to an insufficiency in lysosomal turnover of LC3-II under starvation conditions (Fig. 1B).[14-18] HCV was infected into Huh7.5.1 cells, and the *ATG7* RNAi was performed at day 1 and day 3 post-infection. At day 5 post-infection, cells were harvested, and Atg7 and HCV core, NS3 and NS5A proteins in the cell lysate were analyzed by SDS-PAGE and immunoblotting. Under these conditions, the Atg7 protein was significantly decreased in HCV-infected Huh7.5.1 cells (Fig. 2A). However, the levels of HCV core, NS3 and NS5A proteins in Atg7-knockdown HCV-infected cells remained unchanged as compared with control HCV-infected cells (Fig. 2A). In addition, the levels of HCV mRNA in Atg7-knockdown HCV-infected cells also remained unchanged as compared with control HCV-infected cells (Fig. 2B). These results indicated that the *ATG7* RNAi has little effect on the intracellular production of HCV-related proteins and HCV mRNA.

The next investigation was on whether Atg7-knockdown affects the release of HCV particles. The amount of HCV core protein in the medium at day 5 post-infection was estimated by an ELISA for HCV core antigen. Interestingly, the amount of released HCV core protein derived from Atg7-knockdown cells decreased by about 40 ± 8% compared with control scrambled RNA-treated cells at day 5 post-infection ($p < 0.03$) (Fig. 2E). Under these conditions,

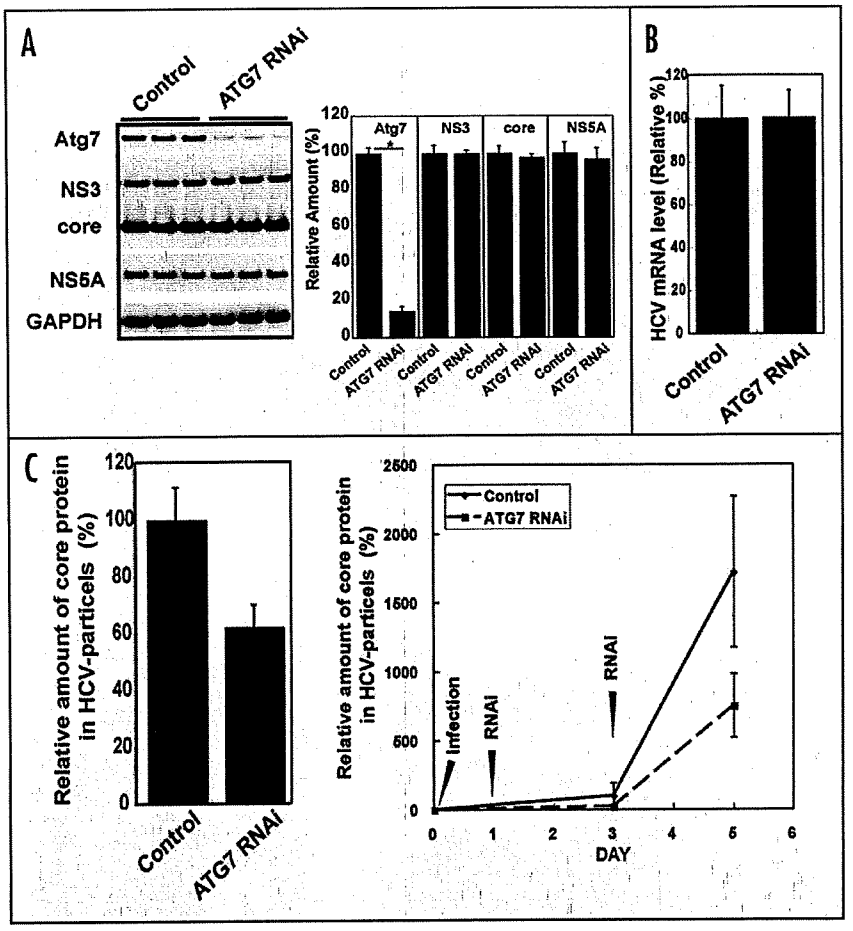

Figure 2. Decrease of infectious HCV particles in the medium by *ATG7*-RNAi. (A) Minor effect of *ATG7* RNAi on the intracellular production of HCV core, NS3 and NS5A proteins. HCV particles were infected into Huh7.5.1 cells. After incubation at 37°C for 2 h, cells were washed and cultured in the DMEM containing 10% fetal calf serum. At day 1 and 3 after HCV infection, dsRNA for *ATG7*-RNAi was transfected into the cells (ATG7 RNAi). As a negative control, scrambled dsRNA was employed (Control). Cells were harvested on day 5 after HCV infection, total proteins (10 μg) were separated by SDS-PAGE, and Atg7, HCV core, NS3 and NS5A proteins in the lysate were recognized by immunoblotting. Three independent experiments are shown. Note that HCV-related proteins remained unchanged, whereas Atg7 protein decreased by the RNAi treatment. Right: indicated the relative levels of intensity of each band estimated by densitometry. Asterisks indicated that the p-value of a Student's t-test is <0.03. The average intensity of "control" in each protein was regarded as 100%. Error bars indicate standard errors. (B) Relative amount of HCV mRNA in Atg7-knockdown cells and control cells. 140 ng of total RNA was used for quantitative RT-PCR. The level of HCV mRNA was normalized by the levels of GAPDH mRNA. Error bars indicate standard errors. (C) Decrease in the amount of the core protein of HCV particle released in the medium by *ATG7*-RNAi. Atg7-knockdown was performed as described in (A). The amount of HCV core protein in HCV particles released into the medium was estimated by a HCV core ELISA kit. The data are from three independent experiments. Relative amount of HCV core protein in Atg7-knockdown cells compared to scrambled RNA infected cells is shown, and the p-value of a Student's t-test is <0.03. Error bars indicate standard errors. Right: indicates the time course of the relative amount of HCV particles. The average amount of HCV particles from control HCV-infected cells at day 3 post-infection was set as 100%.

there was little difference in viability between Atg7-knockdown cells and control cells (Fig. 3A). The amount of HCV mRNA in Huh7.5.1 cells after the reinfection of HCV particles derived from Atg7-knockdown and control cells increased in a time-dependent manner, indicating that the HCV particles derived from Atg7-knockdown cells have a reinfectivity (Fig. 3B). It would be possible that Atg7-knockdown could inhibit the secretory pathway in addition to the release of HCV particles. However, the levels of secreted human albumin, one of the major secreted proteins of hepatocytes, in the medium of Atg7-knockdown cells remained unchanged as compared with that in the medium of control cells, suggesting that there was little, if any, effect on the secretory pathway in HCV-infected cells by the RNAi (Fig. 3C).

To clarify whether or not the decrease of released HCV particles in the medium by *ATG7* RNAi is caused by a defect in autophagy, we investigated the effect of Beclin 1-knockdown on the production of naive HCV-particles (Figs. 3B and C; and 4). Beclin 1, a yeast Atg6 homologue, was isolated as a Bcl-2-interacting protein,[12] and is a subunit of the class III PtdIns 3-kinase lipid-kinase complex essential for autophagy.[19,20] HCV was infected into Huh7.5.1 cells, and *BECN1* RNAi was performed at day 1 and day 3 post-infection. At day 5 post-infection, Beclin 1 protein in HCV-infected Huh7.5.1 cells was knocked down by *BECN1* RNAi compared with scrambled double-stranded RNAs (Fig. 4A). The levels of HCV core, NS3 and NS5A proteins in Beclin 1-knockdown HCV-infected cells remained unchanged as compared with control HCV-infected cells (Fig. 4A). The levels of HCV mRNA in Beclin 1-knockdown HCV-infected cells also remained unchanged as compared with control HCV-infected cells (Fig. 4B). Under these conditions, the amount of released HCV core protein derived from Beclin 1-knockdown cells decreased by about 60 ± 9% compared with control scrambled RNA-treated cells at day 5 post-infection ($p < 0.03$) (Fig. 4C). The HCV particles released from Beclin 1-knockdown cells have reinfectivity (Fig. 3B). There was little difference in viability between Beclin 1-knockdown cells and control cells (Fig. 4D). The levels of secreted human albumin in the medium of Beclin 1-knockdown cells remained unchanged as compared with that in the medium of control cells (Fig. 3C). These results suggested that autophagy contributes to an effective production of infectious HCV particles from the cells without a decrease of the intracellular levels of HCV core, NS3, NS5A or HCV mRNA.

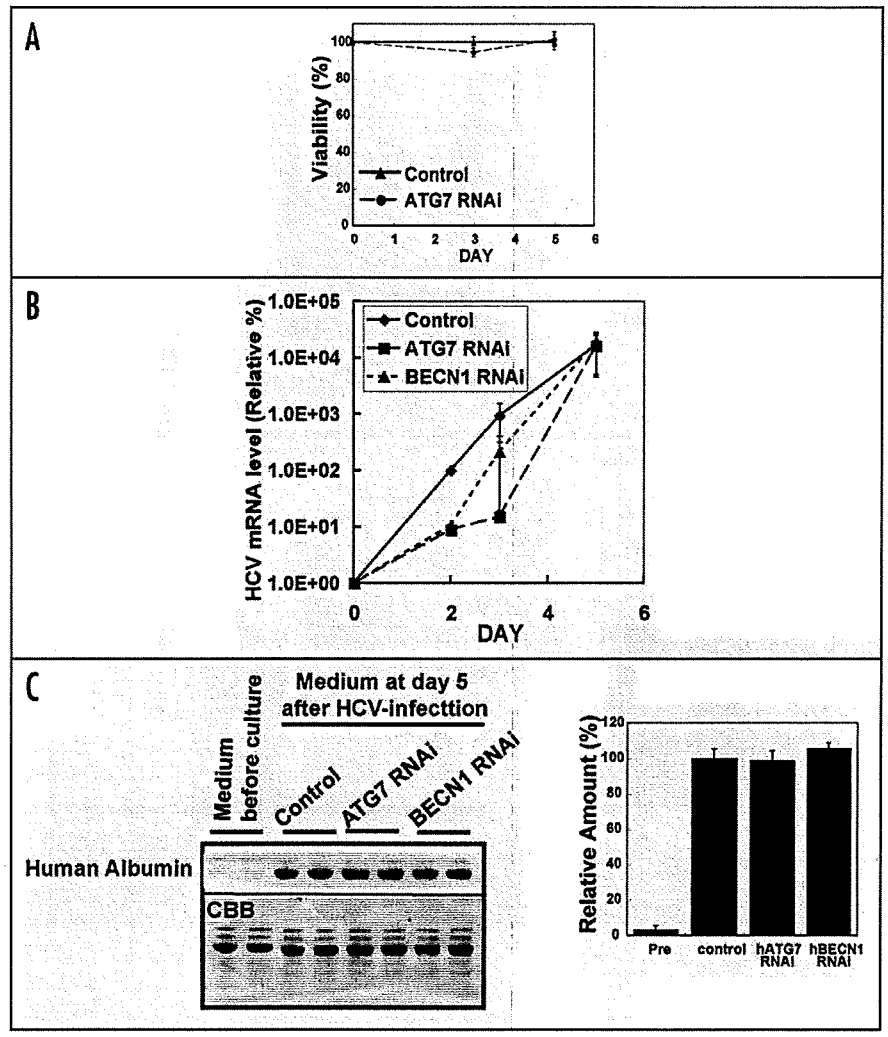

Figure 3. Effects of Atg7-knockdown on cell viability, reinfectivity of HCV particles, and secretion of human albumin. (A) Cell viability of Atg7-knockdown HCV-infected cells. As a negative control for *ATG7* RNAi, scrambled RNA was employed. Error bars indicate standard errors. (B) Reinfectivity of HCV particles derived from Atg7-knockdown HCV-infected cells. HCV-infection, *ATG7*-RNAi and *BECN1*-RNAi were performed as described in Figure 2. At day 5 post-infection, the medium containing HCV particles was harvested. The same volume of the medium containing HCV particles was added to the medium, in which Huh7.5.1 cells were cultured to semiconfluency. After incubation at 37°C for 2 h, cells were washed twice with culture medium, and incubated at 37°C for 2, 3 and 5 days. After RNA-preparation, 140 ng of total RNA was used for quantitative RT-PCR. The level of HCV mRNA was normalized by the levels of GAPDH mRNA. Error bars indicate standard errors. The average amount of HCV mRNA in the control HCV-infected cells at day 2 post-infection was set to 100%. (C) Minor effect of Atg7- and Beclin1-knockdowns on secretion of human albumin in HCV-infected cells. Media from cultured Atg7-(ATG7 RNAi) and beclin1-(BECN1 RNAi) knockdown HCV-infected cells was harvested. As a negative control for RNAi, scrambled RNA was employed (Control). The medium before cell culture was used as a non-incubation control (Medium before culture). Total proteins in the medium were separated by SDS-PAGE, and human albumin in the medium was recognized by immunoblotting with anti-human albumin IgG. To avoid cross-reactivity of the antibody against bovine albumin, the IgG was pre-absorbed with bovine albumin. As a loading control, the membrane was stained with Coomassie Brilliant Blue (CBB). Right: indicates the average relative levels of each bands estimated by densitometry.

Endogenous LC3-puncta displayed little colocalization with HCV core, NS5A or lipid droplets. Intracellular colocalization of endogenous LC3-puncta with HCV core, NS5A and lipid droplets in the HCV-infected cells was investigated next. GFP-LC3-puncta increase in HCV-infected cells.[5-7] However, there are some problems concerning the estimation of autophagy using GFP-LC3.[21-23] Therefore, using affinity purified anti-LC3 IgG, intracellular distribution of endogenous LC3 in the HCV-infected Huh7.5.1 cells was investigated (Figs. 5–9). As positive controls, endogenous LC3 in uninfected Huh7.5.1 cells were stained under starvation conditions in the absence and presence of E64d and pepstatin A (Fig. 6A–F). When uninfected Huh7.5.1 cells were cultured under nutrient-rich conditions, few puncta of LC3 were recognized (Fig. 6A and B). When the uninfected Huh7.5.1 cells were incubated under starvation conditions for 2 h, fluorescence of LC3-positive puncta was increased at a perinuclear region (Fig. 6C and D). The LC3-positive puncta increased in the presence of E64d and pepstatin A under starvation conditions (Fig. 6E and F). In HCV-infected Huh7.5.1 cells, the LC3-positive puncta increased significantly at day 5 post-infection (Figs. 5A vs. 6A, C and E). Deconvolution of high-magnification images (Fig. 8) indicated that LC3-positive puncta in HCV-infected cells were larger than those in starved cells even in the presence of these inhibitors (Fig. 8C and D vs. B). Quantitative analyses of the intensity of the fluorescence of LC3-puncta in each cell indicated that the total intensity of fluorescence of LC3-puncta per cell in HCV-infected cells was about 4.5-fold higher than in uninfected cell under starvation conditions in the presence of E64d and pepstatin A (Fig. 9). Further investigation was made on whether endogenous LC3-puncta colocalized with HCV core, NS5A and lipid droplets. However, there was little colocalization between LC3 and these structures (Figs. 7 and 8).

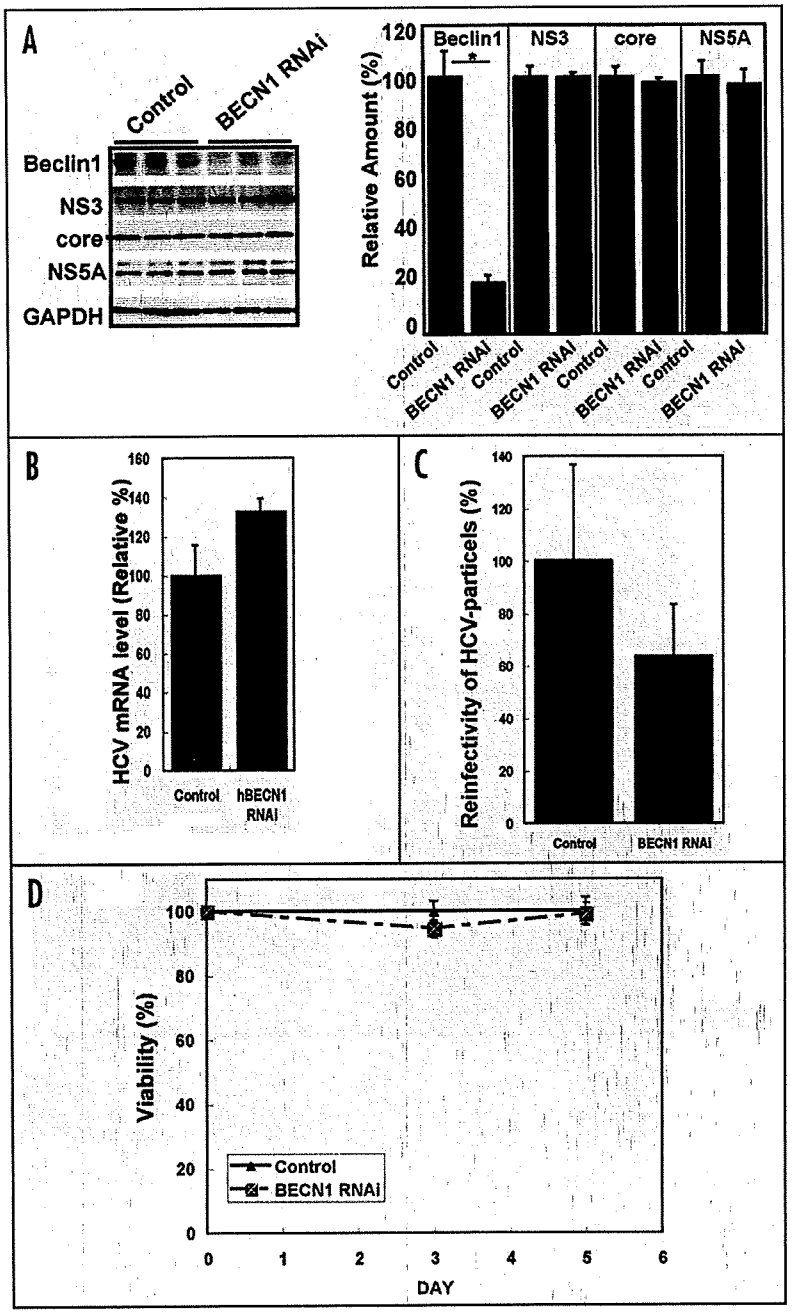

Figure 4. Decrease of infectious HCV particles in the medium by Beclin1 knockdown. (A) Minor effect of Beclin1-knockdown on the intracellular production of HCV core, NS3 and NS5A proteins. HCV-infection, *BECN1* RNAi and immunological analyses were performed as described in Figure 2. BECN1 RNAi, Beclin1-knockdown; Control, scrambled dsRNA. Right: indicates the relative levels of intensity of each band estimated by densitometry. Asterisks indicated that the p-value of a Student's t-test is <0.03. The average intensity of "control" in each protein was set to 100%. Error bars indicate standard errors. (B) Relative amount of HCV mRNA in Beclin1-knockdown cells and control cells. 140 ng of toal RNA was used for quantitative RT-PCR. The level of HCV mRNA was normalized by the levels of ACTB mRNA. Error bars indicate standard errors. (C) Decrease in the amount of the core protein of HCV particle released in the medium by Beclin 1-knockdown. Beclin 1-knockdown-dependent estimation of core protein in HCV particles was performed as described above. The data are from three independent experiments. Relative amount of HCV core protein in Beclin1-knockdown cells compared to scrambled RNA infected cells is shown, and the p-value of a Student's t-test is <0.03. Error bars indicate standard errors. (D) Cell viability of Beclin 1-knockdown HCV-infected cells. As a negative control for *BECN1* RNAi, scrambled RNA was employed. Error bars indicate standard errors.

Discussion

Results of this study showed that Atg7- and Beclin 1-knockdowns in HCV-infected cells resulted in a decrease in the production of infectious HCV particles in the medium, whereas the intracellular production of HCV mRNA and HCV proteins examined remained unchanged. Few endogenous LC3-puncta in HCV-infected cells were colocalized to lipid droplets, core and NS5A proteins.

Using transfection of HCV JFH1 mRNA into Huh7.5 cells, Atg7-knockdown decreases the amount of HCV replicon RNA.[5-7] However, using an in vitro naive HCV JFH1 particle-infection system, Atg7-knockdown decreased the level of infectious particles in the medium by about 40%, whereas intracellular HCV mRNA and HCV proteins remained unchanged. This discrepancy results from the difference between the naive HCV particle-infection system and the transfection of HCV mRNA.

Against some pathogens, autophagy plays a role in intracellular immunity. Initially, it was hypothesized that if autophagy plays a protective role against HCV infection, Atg7- and Beclin 1-knockdowns could lead to an increase of HCV particles and/or intracellular HCV-related proteins. However, contrary to the hypothesis, these knockdowns decreased the production of HCV particles. Atg7 is a key enzyme essential for formation of autophagosomes, and Beclin 1 is a subunit of the class III PtdIns 3-kinase lipid-kinase complex that induces autophagy. Considering that Atg7 and Beclin 1 have different functions in autophagy, these results indicated that autophagy contributes to the effective production of HCV particles in the medium, but little to the intracellular levels of HCV mRNA and HCV-related proteins. It is possible that this knockdown would inhibit the secretory pathway. However, there was little difference in the level of secreted albumin in the medium between autophagy-knockdown cells and control cells. In yeast, no *atg* mutants have defects in the secretory pathway, and there is no report that

ATG gene-knockout influences the secretory pathway in animals and plants. Therefore, it is unlikely that these knockdowns inhibit the secretory pathway. Considering these results, autophagy will contribute to the release and/or assembly of HCV particles, but little to the intracellular production of HCV mRNA and HCV-related proteins.

LC3-II can associate with lipid droplets,[24] and lipid droplets are induced by HCV infection.[4] However, little endogenous LC3-puncta associated with lipid droplets in the HCV-infected Huh7.5.1 cells. These results show that LC3-II cannot always associate with lipid droplets. There is a certain mechanism that allows LC3-II to associate with lipid droplets, which will be the subject of future research.

Materials and Methods

Cells, media, materials and antibodies. Huh7.5.1 cells derived from the Huh7 cell line (ATCC CCL-185) were cultured in Dulbecco's modified Eagle medium (DMEM; Wako, 045-30285) containing 10% fetal calf serum (JRH biosciences/SIGMA, 12603C) and 1% nonessential amino acids (Invitrogen, 11140050). Polyclonal antibodies against Atg7 and LC3 were described previously.[9-11] For the preparation of antiserum against human Beclin 1, rabbits were immunized with a glutathione S-transferase-human Beclin 1 fusion protein. The anti-Beclin 1 IgG was affinity-purified using recombinant human Beclin 1-conjugated Sepharose. The monoclonal antibody against HCV core protein was purchased from Anogen (MO-I40015B), the monoclonal antibody against HCV NS5A protein (HCM-131-5) was from Austral, the monoclonal antibodies against GAPDH (ab8245) and HCV NS3 proteins (ab18664) were from Abcam, and the polyclonal antibody against human albumin (126584) was from Calbiochem. For RNA-interference for human *ATG7* (*ATG7* RNAi) and *BECN1* (*BECN1* RNAi),[12] lipofectamine RNAi MAX, and Stealth™ select RNAi sets (Invitrogen, 1299003), respectively, and Stealth™ RNAi negative control (Invitrogen, 935300) were used. Little interferon mRNAs (IFNA1, IFNA2 and IFNB1) were activated by the transfection of these double-stranded RNAs (Table 1). Protein concentrations were determined using the bicinchoninic acid (BCA) protein assay reagent (Pierce, 23225). E64d (4321-v) and pepstatin A (4397-v) were purchased from Peptide Institute.

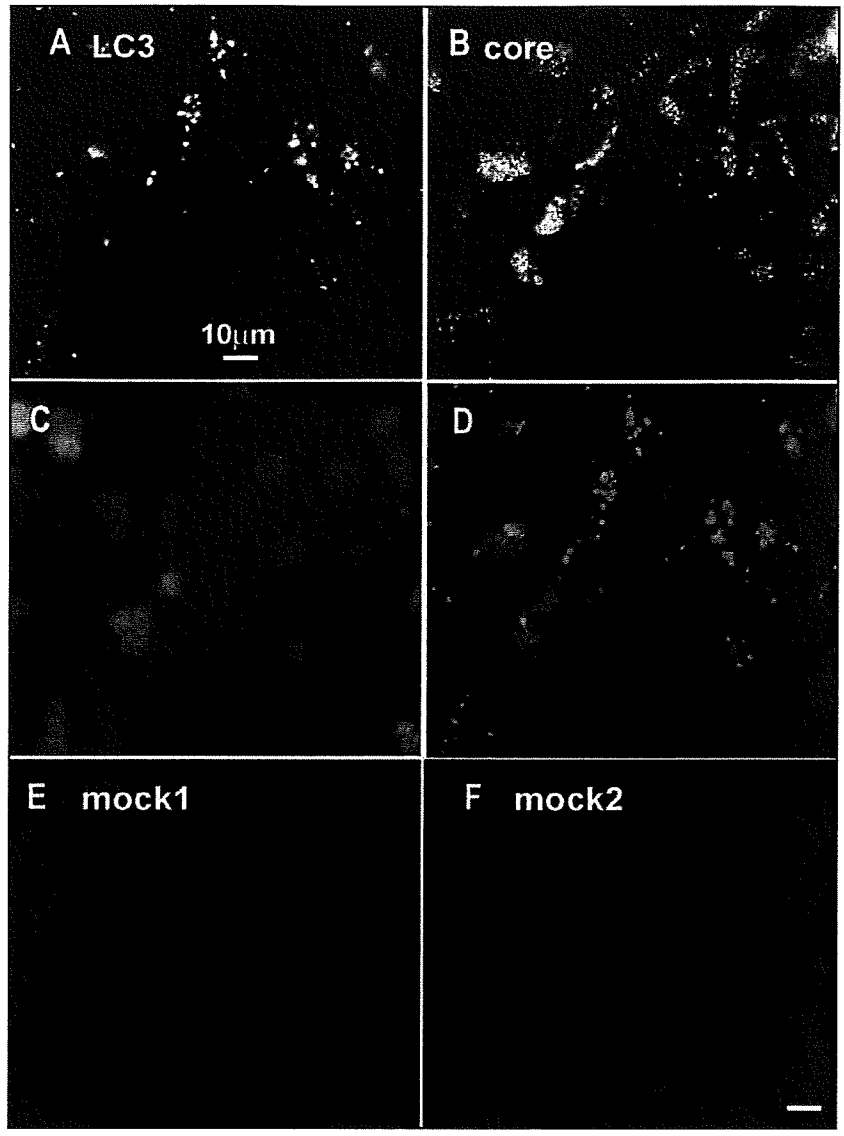

Figure 5. Intracellular distribution of endogenous LC3 in HCV-infected Huh7.5.1 cells. Cells were fixed in 4% paraformaldehyde/PBS at day 5 post-infection (A–F), and permeabilized in 50 μg/ml of digitonin. Endogenous LC3 in the cells was recognized with rabbit anti-LC3 IgG and Alexa488-conjugated goat anti-rabbit IgG (A). Intracellular HCV core protein was recognized with mouse anti-HCV core IgG and Alexa594-conjugated goat ant-mouse IgG (B). DAPI staining was in (C). As a negative control for LC3-staining, cells were stained with normal rabbit IgG and Alexa488-conjugated goat anti-rabbit IgG (E mock 1). As a negative control for HCV core-staining, cells were stained with normal mouse IgG and Alexa594-conjugated goat anti-mouse IgG (F mock 2). Fluorescence of Alexa488, Alexa594 and DAPI was monitored by fluorescence microscopy. Merged pseudo color images (LC3, green: HCV core, red: and DAPI, blue) was shown in (D). Bars indicate 10 μm.

Infection of Huh7.5.1 cells with HCV. Infectious HCV (JFH1 strain) particles were produced in Huh7.5.1 cells as described in an earlier study.[13] Culture supernatant containing infectious HCV particles was collected and stored at -80°C until use. Subconfluent Huh7.5.1 cells in 24-well or 48-well plates were exposed to

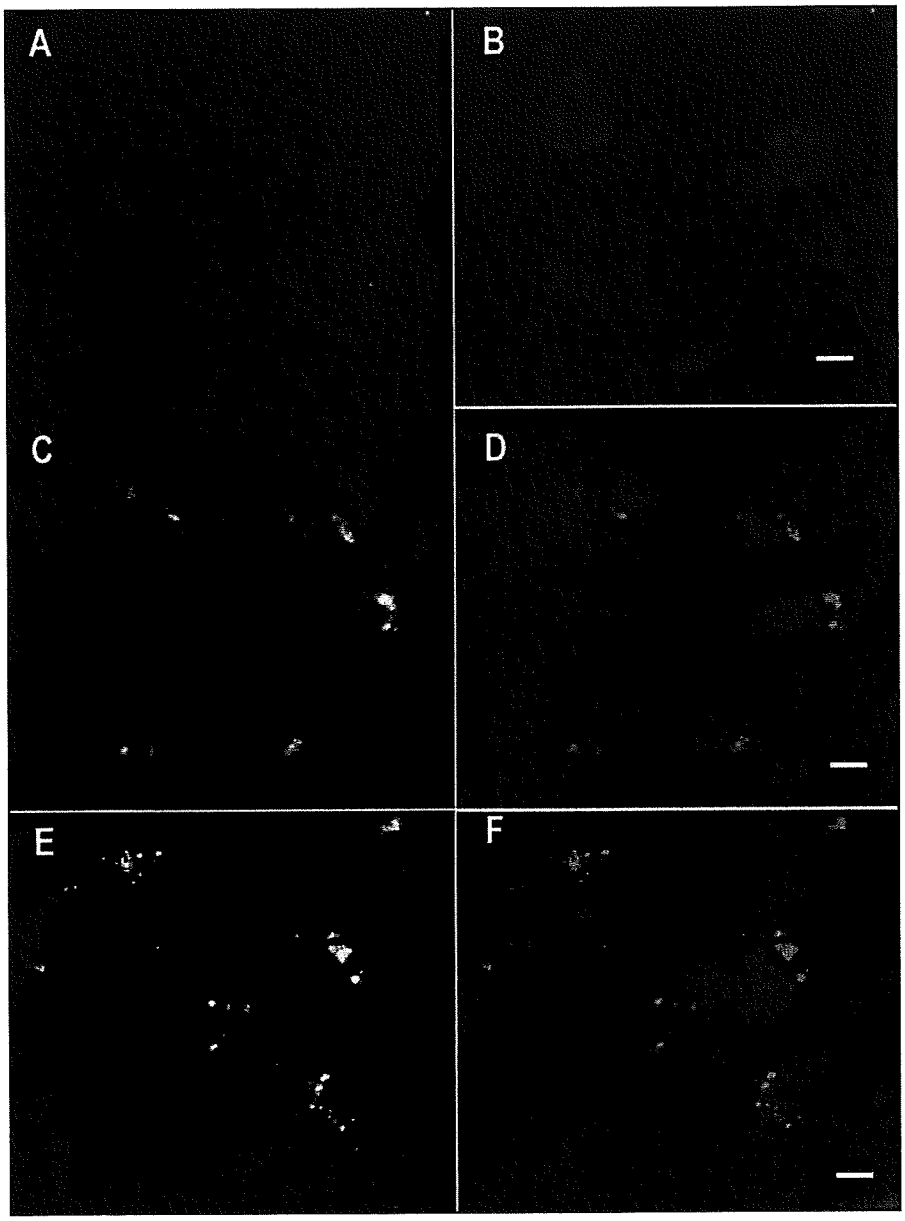

Figure 6. Intracellular distribution of endogenous LC3 in starved Huh7.5.1 cells. Huh7.5.1 cells were cultured in the nutrient-rich medium (A and B). For starvation-induced autophagosomes and autolysosomes, cells were incubated in the Krebs-Ringer buffered medium for 4 h in the absence (C and D) or presence (E and F) of E64d and pepstatin A. Endogenous LC3 in the cells was recognized with rabbit anti-LC3 IgG and Alexa488-conjugated goat anti-rabbit IgG (A, C and E). Merged pseudo color images (LC3, green: and DAPI, blue) were shown in (B, D and E). Bars indicate 10 μm.

normal culture medium containing HCV particles (8 fmoles of core protein/well, corresponding to moi = 0.1) for 6 h at 37°C. Cells were then washed and maintained in 500 μl (24-well) or 250 μl (48-well) of normal culture medium for 6–7 days at 37°C. To determine HCV production activity, the amounts of HCV core protein in the culture medium was quantified with an enzyme-linked immunosorbent assay (ELISA) (Ortho® HCV antigen ELISA test, Ortho-Clinical Diagnostics, 601002).

Immunoblotting analyses. After HCV infection, cells were washed twice in phosphate-buffered saline, lysed in lysis buffer (10 mM sodium phosphate, pH 7.2, 150 mM NaCl, and 1% sodium dodecyl sulfate) containing a Complete® protease-inhibitor cocktail (Roche Diagnostics, 1697498). Proteins (10 μg) of the lysate were separated on sodium dodecyl sulfate polyacrylamide gel electrophoresis (SDS-PAGE) (4–12% Bis-Tris, Invitrogen, NP0322BOX). After transferring the proteins to a polyvinylidine difluoride membrane using a Trans-Blot SD transfer cell (Bio-Rad, 170-3940), HCV core protein, HCV NS3 protein, HCV NS5A protein, and Atg7 in the lysate were recognized with appropriate antibodies. A chemiluminescent method was carried out according to standard protocols with SuperSignal West Dura Extended Duration Substrate (Pierce, 34075) or SuperSignal West Pico Chemiluminescent Substrate (Pierce, 34077).

Immunofluorescence analyses. Indirect immunofluoresence analysis was basically performed as described in the literature.[11,14] Briefly, cells were fixed in a fixation solution (phosphate buffered saline containing 4% paraformaldehyde) at room temperature for 5 min, and permeabilized in phosphate-buffered saline containing 1% digitonin. Rabbit polyclonal anti-LC3 antibody (10 μg/ml), mouse monoclonal anti-HCV core antibody (10 μg/ml), and mouse monoclonal anti-HCV NS5A antibody were used for recognizing LC3, HCV core protein, and HCV NS5A protein, respectively. As secondary antibodies, Alexa488-conjugated goat anti-rabbit IgG (Invitrogen, A11008) and Alexa594-conjugated goat anti-mouse IgG (Invitrogen, A11005) were used. Nile Red (Invitrogen, N1142) was used for lipid droplet staining. Fluorescence of Alexa488 and Alexa594 was monitored with Biozero BZ-8000 (KEYENCE, Tokyo, Japan).

Other techniques. Densitometric analyses of images were performed with an ImageJ program (http://rsbweb.nih.gov/ij/) on a PowerMac G4 computer. Cell viability was measured with a CellTiter 96 nonradioactive cell proliferation assay kit (Promega,

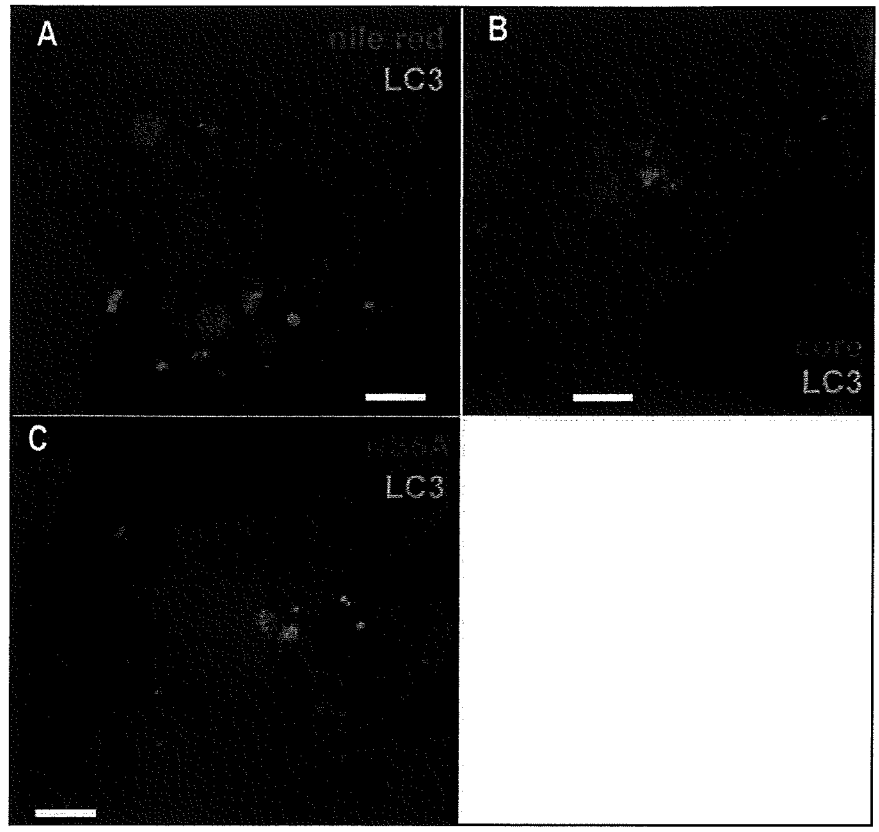

Figure 7. Minor colocalization of LC3 with lipid droplets, HCV core or HCV NS5A proteins. Lipid droplets in HCV-infected cells were stained nile red (A, pseudo color is red), HCV core proteins were stained with mouse anti-HCV core antibody and Alexa594-conjugated goat anti-mouse IgG (B, pseudo color is red), and HCV NS5A proteins were stained with mouse anti-HCV NS5A antibody and Alexa594-conjugated goat anti-mouse IgG (C, pseudo color is red). Pseudo color of LC3 is green in (A–C). Merged images are shown. Bars indicate 5 μm.

G4000). Total RNA was prepared by a RNeasy plus mini kit (Qiagen, 74134). Quantitative RT-PCR of mRNA was performed with a Lightcycler480 using a Lightcycler RNA Master SYBR Green I kit (Roche, 3064760).

Acknowledgements

This study was supported in part by grants-in-aid from the Ministry of Health, Labor and Welfare of Japan, and by a grant from the Mochida Memorial Foundation for Medical and Pharmaceutical Research (to I.T.), and by Grants-in-Aid for Scientific Research on Priority Areas "Proteolysis in the Regulation of Biological Processes" from the Ministry of Education, Science, Sports and Culture of Japan (to I.T.).

References

1. Liang TJ, Rehermann B, Seeff LB, Hoofnagle JH. Pathogenesis, natural history, treatment and prevention of hepatitis C. Ann Intern Med 2000; 132:296-305.
2. Reed KE, Rice CM. Overview of hepatitis C virus genome structure, polyprotein processing and protein properties. Curr Top Microbiol Immunol 2000; 242:55-84.
3. Egger D, Wolk B, Gosert R, Bianchi L, Blum HE, Moradpour D, Bienz K. Expression of hepatitis C virus proteins induces distinct membrane alterations including a candidate viral replication complex. J Virol 2002; 76:5974-84.
4. Miyanari Y, Atsuzawa K, Usuda N, Watashi K, Hishiki T, Zayas M, et al. The lipid droplet is an important organelle for hepatitis C virus production. Nat Cell Biol 2007; 9:1089-97.
5. Sir D, Chen WL, Choi J, Wakita T, Yen TS, Ou JH. Induction of incomplete autophagic response by hepatitis C virus via the unfolded protein response. Hepatology 2008; 48:1054-61.
6. Sir D, Liang C, Chen WL, Jung JU, Ou JH. Perturbation of autophagic pathway by hepatitis C virus. Autophagy 2008; 4:830-1.
7. Ait-Goughoulte M, Kanda T, Meyer K, Ryerse JS, Ray RB, Ray R. Hepatitis C virus genotype 1a growth and induction of autophagy. J Virol 2008; 82:2241-9.
8. Fujimoto T, Ohsaki Y. Proteasomal and autophagic pathways converge on lipid droplets. Autophagy 2006; 2:299-301.
9. Tanida I, Tanida-Miyake E, Ueno T, Kominami E. The human homolog of *Saccharomyces cerevisiae* Apg7p is a Protein-activating enzyme for multiple substrates including human Apg12p, GATE-16, GABARAP and MAP-LC3. J Biol Chem 2001; 276:1701-6.
10. Asanuma K, Tanida I, Shirato I, Ueno T, Takahara H, Nishitani T, et al. MAP-LC3, a promising autophagosomal marker, is processed during the differentiation and recovery of podocytes from PAN nephrosis. FASEB J 2003; 17:1165-7.
11. Tanida I, Ueno T, Kominami E. LC3 and Autophagy. Methods Mol Biol 2008; 445:77-88.
12. Liang XH, Jackson S, Seaman M, Brown K, Kempkes B, Hibshoosh H, Levine B. Induction of autophagy and inhibition of tumorigenesis by *beclin 1*. Nature 1999; 402:672-6.
13. Wakita T, Pietschmann T, Kato T, Date T, Miyamoto M, Zhao Z, et al. Production of infectious hepatitis C virus in tissue culture from a cloned viral genome. Nat Med 2005; 11:791-6.
14. Tanida I, Minematsu-Ikeguchi N, Ueno T, Kominami E. Lysosomal turnover, but not a cellular level, of endogenous LC3 is a marker for autophagy. Autophagy 2005; 1:84-91.
15. Bjørkøy G, Lamark T, Brech A, Outzen H, Perander M, Øvervatn A, et al. p62/SQSTM1 forms protein aggregates degraded by autophagy and has a protective effect on huntingtin-induced cell death. J Cell Biol 2005; 171:603-14.
16. Komatsu M, Waguri S, Ueno T, Iwata J, Murata S, Tanida I, et al. Impairment of starvation-induced and constitutive autophagy in Atg7-deficient mice. J Cell Biol 2005; 169:425-34.
17. Komatsu M, Waguri S, Chiba T, Murata S, Iwata J, Tanida I, et al. Loss of autophagy in the central nervous system causes neurodegeneration in mice. Nature 2006; 441:880-4.
18. Komatsu M, Waguri S, Koike M, Sou YS, Ueno T, Hara T, et al. Homeostatic levels of p62 control cytoplasmic inclusion body formation in autophagy-deficient mice. Cell 2007; 131:1149-63.
19. Levine B, Kroemer G. Autophagy in the pathogenesis of disease. Cell 2008; 132:27-42.
20. Levine B, Sinha S, Kroemer G. Bcl-2 family members: dual regulators of apoptosis and autophagy. Autophagy 2008; 4:600-6. Epub 2008.
21. Kuma A, Matsui M, Mizushima N. LC3, an Autophagosome Marker, Can be Incorporated into Protein Aggregates Independent of Autophagy: Caution in the Interpretation of LC3 Localization. Autophagy 2007; 3:4.
22. Katayama H, Yamamoto A, Mizushima N, Yoshimori T, Miyawaki A. GFP-like proteins stably accumulate in lysosomes. Cell Struct Funct 2008; 33:1-12.
23. Tanida I, Yamaji T, Ueno T, Ishiura S, Kominami E, Hanada K. Consideration about negative controls for LC3 and expression vectors for four colored fluorescent protein-LC3 negative controls. Autophagy 2008; 4:131-4.
24. Ohsaki Y, Cheng J, Fujita A, Tokumoto T, Fujimoto T. Cytoplasmic lipid droplets are sites of convergence of proteasomal and autophagic degradation of apolipoprotein B. Mol Biol Cell 2006; 17:2674-83.

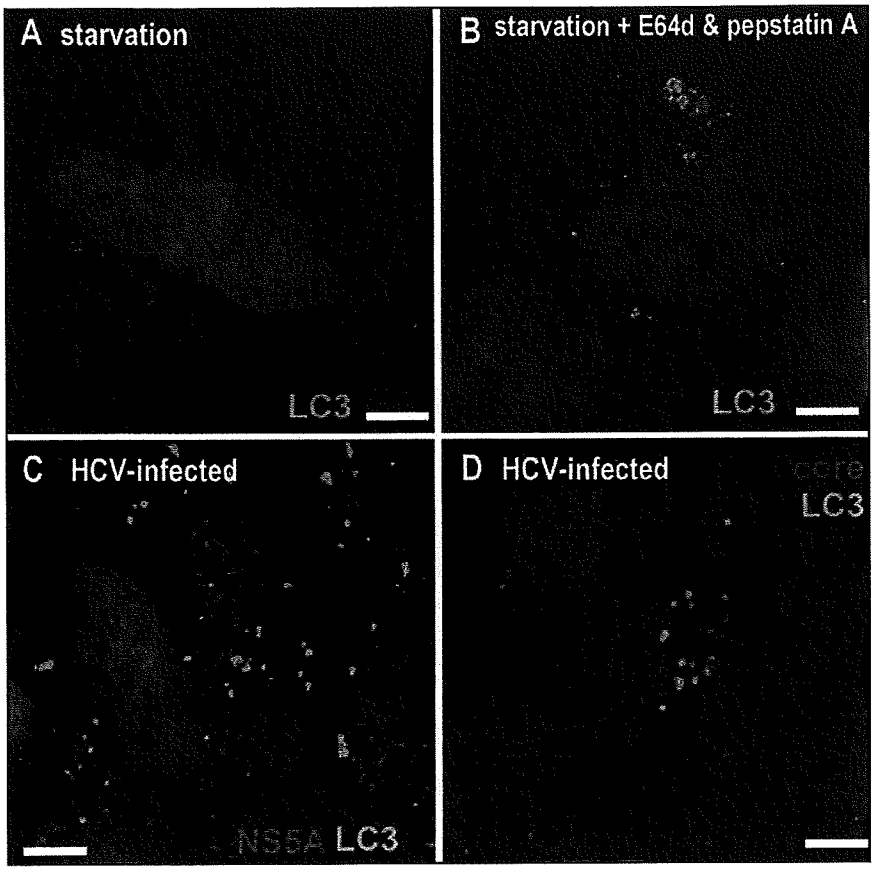

Figure 8. Deconvoluted images of LC3, core and NS5A in HCV-infected Huh7.5.1 cells. The fluorescence images of endogenous LC3 (A–D, pseudo color is green), NS5A (C, pseudo color is red), and core (D, pseudo color is red) were obtained by fluorescent microscopy. The images were deconvoluted with ImageJ program (http://rsbweb.nih.gov/ij/) and a plug-in for iterative deconvolution (http://www.optinav.com/Iterative-Deconvolution.htm). Pseudo color for DAPI staining is blue. Merged images are shown. Note that the size of LC3-puncta in HCV-infected cells (C and D) were larger than under starvation conditions in the absence (A) or presence (B) of E64d and pepstatin A.

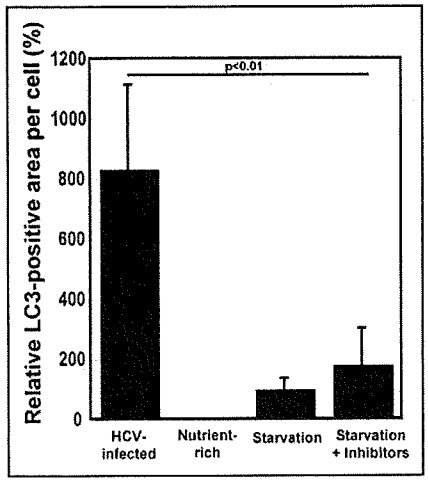

Figure 9. Increase of the fluorescence of LC3 in HCV-infected cells. The images of fluorescence of LC3 were analyzed with an ImageJ program (http://rsbweb.nih.gov/ij/) and plug-ins for iterative deconvolution (http://www.optinav.com/Iterative-Deconvolution.htm) and tophat-filter (http://rsb.info.nih.gov/ij/plugins/lipschitz/). The fluorescent images of over 200 cells were analyzed, and relative intensity was calculated; the average intensity of LC3 in Huh7.5.1 cell under starvation conditions (starvation) in the absence of E64d and pepstatin A was set to 100%.

Table 1 **Little mRNAs of interferons were activated by *ATG7*- and *BECN1*-RNAi**

	IFNA1	*IFNA2*	*IFNB1*
	(copies of mRNA/100 ng total RNA)		
Uninfected Huh7	5.6 ± 1.5	0.8 ± 0.1	0.4 ± 0.1
HCV-infected/scrambled RNA	5.8 ± 5.0	1.8 ± 0.1	4.9 ± 3.6
HCV-infected/*ATG7* RNAi	0.6 ± 0.1	1.3 ± 0.3	0.9 ± 0.5
HCV-infected/*BECN1* RNAi	0.3 ± 0.1	1.1 ± 0.2	2.1 ± 1.3

HCV was infected into Huh7.5.1 cells, and RNA interference was performed at day 1 and day 3 post-infection (HCV-infected). At day 5 post-infection, total RNA was prepared with a RNeasy plus kit. As a negative control for RNAi, scrambled RNA was employed. As a negative control for HCV-infection, Huh7 cells were incubated for 5 days (Uninfected Huh7), and total RNA was prepared. Quantitative RT-PCR of mRNA was performed with a Lightcycler480 (Roche) with appropriate primer-sets for each genes.

Virology 383 (2009) 319–327

Contents lists available at ScienceDirect

Virology

journal homepage: www.elsevier.com/locate/yviro

Cellular vimentin content regulates the protein level of hepatitis C virus core protein and the hepatitis C virus production in cultured cells

Yuko Nitahara-Kasahara [a,1], Masayoshi Fukasawa [a,*], Fumiko Shinkai-Ouchi [a], Shigeko Sato [a], Tetsuro Suzuki [b], Kyoko Murakami [b], Takaji Wakita [b], Kentaro Hanada [a], Tatsuo Miyamura [c], Masahiro Nishijima [a,d]

[a] Department of Biochemistry and Cell Biology, National Institute of Infectious Diseases, 1-23-1, Toyama, Shinjuku-ku, Tokyo 162-8640, Japan
[b] Department of Virology II, National Institute of Infectious Diseases, Tokyo 162-8640, Japan
[c] National Institute of Infectious Diseases, Tokyo 162-8640, Japan
[d] National Institute of Health Sciences, Tokyo 158-8501, Japan

ARTICLE INFO

Article history:
Received 14 August 2008
Returned to author for revision
3 September 2008
Accepted 6 October 2008
Available online 14 November 2008

Keywords:
Hepatitis C virus
Core protein
Vimentin

ABSTRACT

Hepatitis C virus (HCV) core protein is essential for virus particle formation. Using HCV core-expressing and non-expressing Huh7 cell lines, Uc39-6 and Uc321, respectively, we performed comparative proteomic studies of proteins in the 0.5% Triton X-100-insoluble fractions of cells, and found that core-expressing Uc39-6 cells had much lower vimentin content than Uc321 cells. In experiments using vimentin-overexpressing and vimentin-knocked-down cells, we demonstrated that core protein levels were affected by cellular vimentin content. When vimentin expression was knocked-down, there was no difference in mRNA level of core protein; but proteasome-dependent degradation of the core protein was strongly reduced. These findings suggest that the turnover rate of core protein is regulated by cellular vimentin content. HCV production was also affected by cellular vimentin content. Our findings together suggest that modulation of hepatic vimentin expression might enable the control of HCV production.

Introduction

Hepatitis C virus (HCV) is a major causative agent of chronic hepatitis (Choo et al., 1989; Kuo et al., 1989). Persistent HCV infection, which develops in at least 70% of infected patients, is strongly correlated with the development of severe liver diseases such as fibrosis, steatosis, cirrhosis, and hepatocellular carcinomas (HCC). Since more than 170 million people in the world are currently infected with HCV (Choo et al., 1989) and there is no treatment completely effective in curing HCV, HCV infection is one of the most important global public health issues. Understanding of the life cycle of HCV and the mechanism by which HCV induces serious liver diseases is crucial for the development of novel anti-HCV strategies.

HCV is an RNA virus of the *Flaviviridae* family and possesses a single-stranded, positive-sense RNA genome of ~9.6 kb (Bartenschlager and Lohmann, 2000). The HCV RNA genome encodes a polyprotein of ~3000 amino acids that is processed by host and viral proteases into 10 individual components including 4 structural and 6 nonstructural proteins (reviewed by Reed and Rice, 2000). HCV core protein is crucial for virus particle production as the structural component of the viral nucleocapsid and as a unit required for formation of the active HCV replication/assembly complex in host cells (Boulant et al., 2007; Miyanari et al., 2007). In addition, the core protein plays pivotal roles in the pathogenesis of HCV infection, as suggested by the finding that transgenic mice expressing core protein in the liver tend to develop liver steatosis with subsequent HCC (Moriya et al., 1998; Moriya et al., 1997). A large number of studies have revealed that a variety of host proteins interact with the core protein (Suzuki et al., 2007). Although these interactions can markedly affect various biological functions in host cells, it is not clearly known yet which interactions and molecules play roles in HCV production or its pathogenicity. Recent exhaustive gene-silencing analyses of host factors using RNAi demonstrated that RNA helicase DDX3, one of the proteins that interacts with the core, is required for HCV RNA replication as well as HCV production (Ariumi et al., 2007; Randall et al., 2007).

In host hepatic cells, HCV core protein is distributed preferentially in the detergent-resistant fractions (Matto et al., 2004), and HCV RNA replication also occurs on detergent-resistant membranes (Aizaki et al., 2004; Shi et al., 2003), suggesting that host factors in the detergent-resistant fractions play roles in core protein functions. In this study, we focused on HCV core protein and the detergent-insoluble proteins of host cells, and performed comparative targeted proteomic analysis of the detergent-insoluble proteins in HCV core-expressing and non-expressing hepatic cells. We identified vimentin as a protein the amount of which was reduced in core-expressing cell lines, and demonstrated that cellular vimentin content affects levels of HCV core protein through the proteasome-mediated protein

* Corresponding author. Fax: +81 3 5285 1157.
E-mail address: fuka@nih.go.jp (M. Fukasawa).
[1] Present address: National Institute of Neuroscience, National Center of Neurology and Psychiatry, Tokyo 187-8502, Japan.

0042-6822/$ – see front matter © 2008 Published by Elsevier Inc.
doi:10.1016/j.virol.2008.10.009

degradation system. Since cellular vimentin levels ultimately affected HCV production, vimentin may be a novel target for strategies of anti-HCV treatment.

Results

Proteomic analysis of detergent-insoluble fractions (DISFs) by second-dimensional polyacrylamide gel electrophoresis (2D-PAGE)/MALDI-QIT-TOF MS

DISFs and detergent-soluble fractions (DSFs) were prepared from HCV core-expressing Uc39-6 and non-expressing Uc321 cells by a sucrose density gradient ultracentrifugation method as described in Materials and methods. Proteins in the DISFs and DSFs were analyzed by immunoblotting with antibodies to HCV core protein and various organelle markers (Fig. 1A). A significant amount of HCV core protein (~70%) was distributed in the DISF of Uc39-6 cells. Nuclear proteins such as laminA/C and laminB were concentrated only in the DISFs of both types of cells, whereas other organelle proteins such as annexin II (plasma membrane), fatty acid synthase (cytosol), prohibitin (mitochondria), and calnexin (endoplasmic reticulum) were detected in the DSFs but not DISFs (Fig. 1A), suggesting that the DISFs in both types of cells contain minor (~15%) discrete populations of cellular proteins. Next, we performed 2D-PAGE analysis of the DISFs in Uc321 and Uc39-6 cells. Proteins in the DISFs were separated by isoelectric focusing (IEF) (pH 4–7) and 12% sodium dodecyl sulfate (SDS)-PAGE, and visualized by SYPRO-Ruby staining (Fig. 1B). Intensity of each spot in 2-D images was compared between Uc321 and Uc39-6 cells. The most difference in DISF proteins between Uc321 and Uc39-6 cells (the Uc39-6/Uc321 ratios of intensity normalized with actin: 10.8–28.0) was detected in the spots numbered as 1 in Fig. 1B (MW~57 kDa, p*I*~4.7), in which vimentin alone was identified by mass spectrometric analysis. We therefore focused on the relationship between cellular vimentin and core protein in further investigations.

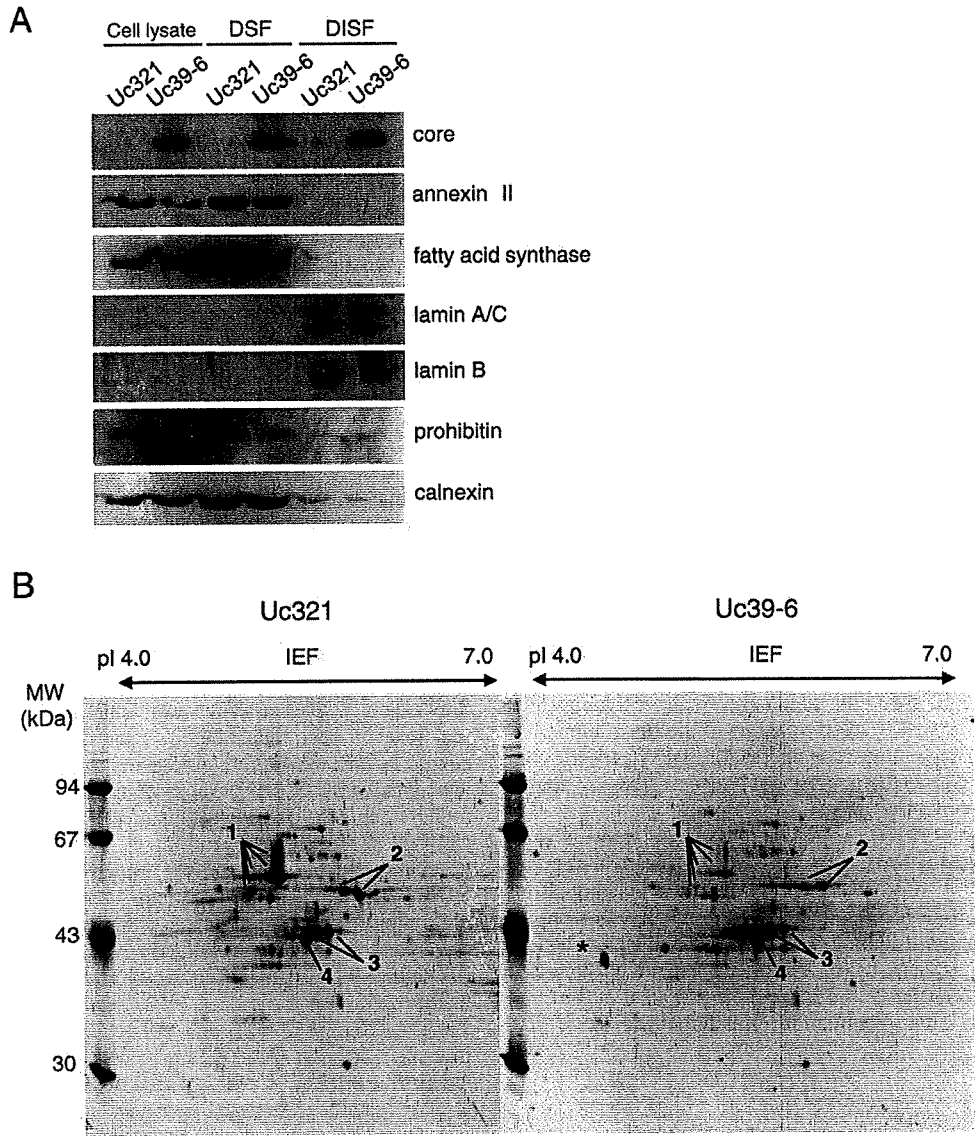

Fig. 1. Immunoblot and 2D-PAGE analysis of DISFs. (A) Total cell lysate fractions (5 μg of protein), DSFs (50 μg of protein), and DISFs (5 μg of protein) from core-expressing Uc39-6 and non-expressing Uc321 cells were analyzed by immunoblotting with antibodies to HCV core protein and various organelle markers as indicated. (B) 2D-PAGE analysis of proteins in DISFs of Uc321 and Uc39-6 cells. Proteins (150 μg) were separated by IEF (pH 4–7), followed by SDS-PAGE on a 12% gel. The gels were stained with SYPRO-Ruby. Major spots, identified as cytoskeletal proteins, are marked: 1, vimentin; 2, cytokeratin 8; 3, cytokeratin 18; 4, actin. *: a non-specific spot.

HCV core-expressing cell lines exhibited reduced vimentin content

To confirm the reduction of vimentin levels in DISFs of HCV core-expressing Uc39-6 cells, immunoblot analysis was performed using anti-vimentin antibody. Uc39-6 cells exhibited lower vimentin contents not only in DISF but also the total cell lysate fraction compared with control Uc321 cells (Fig. 2A). Similar results were obtained in the cell lysate fraction of another independent clone of an HCV core-expressing Huh7 cell line, Uc39-2 (Fig. 2B). Furthermore, a core-expressing hepatic HepG2 cell line, Hep39, also had lower vimentin content than a control cell line, Hepswx (Fig. 2C). These findings exclude the possibility that the reduction of vimentin levels in core-expressing cell lines is a clone- or cell-specific event. Consistent with these findings, levels of vimentin mRNA in Uc39-2 and Uc39-6 cells were also lower than that in Uc321 cells (data not shown). Taken together, these findings demonstrate marked reduction of vimentin expression in HCV core-expressing cell lines.

Cellular vimentin content affects the protein level of HCV core protein

To investigate the relationship between HCV core protein and vimentin, we examined the effect of cellular vimentin content on level of HCV core protein. When the expression of vimentin or control hypoxanthine guanine phosphoribosyltransferase 1 (HPRT) was knocked down in Uc39-6 cells by siRNA treatment, the protein level of HCV core protein in vimentin-knocked-down cells was significantly higher than those in siRNA-untreated and HPRT-knocked-down cells (Fig. 3A). On the other hand, cellular mRNA levels of HCV core protein, corrected for β-actin mRNA content, did not differ substantially among these types of cells (Table 1). These findings revealed that post-translational steps were involved in the increase of HCV core protein level in vimentin-knocked-down cells. Next, we established a vimentin-overexpressing Huh7 cell line, Huh7/vimentin, and compared the level of the core protein in Huh7/vimentin cells with that in control Huh7/hygro cells after transient expression of the core protein with pcEF39neo vector. After 9-day culture with G418 selection, the viabilities of the two types of cells were similar, though the level of expression of the core protein in Huh7/vimentin was significantly lower than that in Huh7/hygro cells (Fig. 3B). These findings demonstrated that level of HCV core protein was inversely correlated with cellular vimentin content, and thus strongly suggested that it was affected by cellular vimentin content.

We further attempted to verify these effects of vimentin using the vimentin-null cell line 1HF5 and the vimentin-expressing control cell line 2CB5, derived from human adrenal carcinoma SW13 cells (Sarria et al., 1990). When 1HF5 and 2CB5 cells were transfected with the core expression vector pcEF39neo and cultured with G418 selection, the viabilities of the two types of cells were similar, though the level of expression of the core protein in 1HF5 cells was much higher than that in 2CB5 cells (Fig. 3C), consistent with the results in Figs. 3A, B. An exogenously vimentin-expressing 1HF5 cell line carrying pcDNA3.1/Hygro/vimentin, 1HF5/vimentin, and a control vimentin-null cell line carrying pcDNA3.1/Hygro, 1HF5/hygro, were then established, and transfected with the green fluorescent protein (GFP)-expressing pcDNA3.1/EGFP vector, the core-coding pcEF39neo vector, or the control pcFE321swxneo vector. After selection under G418 for 9 days, the viabilities of these transfected cells were nearly the same. The levels of expression of GFP were similar in 1HF5/hygro and 1HF5/vimentin cells, while the core protein level in 1HF5/vimentin cells was significantly lower than that in 1HF5/hygro cells (Fig. 3D), consistent with the results in Fig. 3B.

These findings together indicate that cellular vimentin content regulates the level of HCV core protein in post-translational fashion.

Vimentin is involved in proteasomal degradation of core proteins in cells

HCV core proteins are known to be preferentially degraded by the proteasome-dependent pathway (Suzuki et al., 2001). To determine whether cellular vimentin content affects proteasome-dependent degradation of the core protein, we examined the effects of the proteasome inhibitor MG132 on core protein levels in vimentin-knocked-down cells. After Huh7 cells transfected with pCAG/Flag-core (Huh7/Flag-core cells) had been treated with MG132 for 16 h, cellular accumulation of core protein was analyzed by immunoblot (Fig. 4; lanes 3 vs 4), which indicated substantial proteasomal degradation of the core proteins in cultured cells, as described previously (Hope and McLauchlan, 2000; McLauchlan et al., 2002; Suzuki et al., 2001). Huh7/Flag-core cells transfected with control and HPRT siRNA duplexes exhibited similar increases in core protein levels by treatment with MG132 (Fig. 4; lanes 5 vs 6, and 9 vs 10). On the other hand, vimentin-knocked-down Huh7/Flag-core cells that were transfected with vimentin siRNA duplexes exhibited higher content of core protein (lane 7) than the other siRNA-treated cells (lanes 5 and 9), and MG132 treatment resulted in no significant difference in core protein levels in vimentin-knocked-down cells (lanes 7 and 8), indicating that proteasomal degradation of core proteins was markedly inhibited in the vimentin-knocked-down cells. These observations strongly suggested that vimentin plays an important role in the proteasome-mediated proteolytic pathway of the HCV core protein.

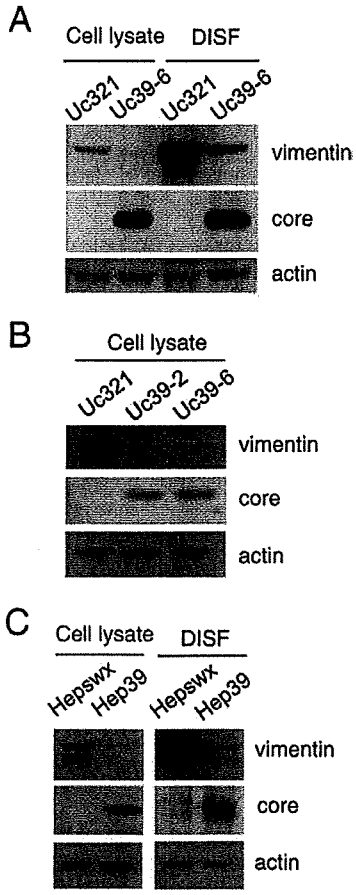

Fig. 2. Immunoblot analysis of vimentin in HCV core-expressing cell lines. Cell lysate fractions and DISFs from various cell lines were analyzed by immunoblotting with antibodies to vimentin, HCV core protein, and β-actin as indicated: cell lysate fractions and DISFs from Uc321 and Uc39-6 cells in (A), cell lysate fractions from Uc321, Uc39-2, and Uc39-6 cells in (B), and cell lysate fractions and DISFs from Hepswx and Hep39 cells in (C). Amounts of protein loaded were 18 μg in (A) and (B), and 5 μg in (C).